Year-round CH4 and CO2 flux dynamics in two contrasting freshwater ecosystems of the subarctic

Jammet, Mathilde; Dengel, Sigrid; Kettner, Ernesto; Parmentier, Frans-Jan W.; Wik, Martin; Crill, Patrick; Friborg, Thomas

Biogeosciences

Year-round CH$_4$ and CO$_2$ flux dynamics in two contrasting freshwater ecosystems of the subarctic

Mathilde Jammet[1], Sigrid Dengel[2], Ernesto Kettner[1], Frans-Jan W. Parmentier[3], Martin Wik[4], Patrick Crill[4], and Thomas Friborg[1]

[1]Center for Permafrost (CENPERM), Department for Geosciences and Natural Resource Management,
University of Copenhagen, Copenhagen, 1350, Denmark
[2]Climate and Ecosystem Sciences Division, Lawrence Berkeley National Laboratory, Berkeley, CA 94720, USA
[3]Department of Arctic and Marine Biology, UiT – The Arctic University of Norway, Postboks 6050 Langnes,
9037 Tromsø, Norway
[4]Department of Geological Sciences, Stockholm University, Stockholm, 106 91, Sweden

Correspondence to: Mathilde Jammet (mathilde.jammet@ign.ku.dk)

Abstract. Lakes and wetlands, common ecosystems of the high northern latitudes, exchange large amounts of the climate-forcing gases methane (CH$_4$) and carbon dioxide (CO$_2$) with the atmosphere. The magnitudes of these fluxes and the processes driving them are still uncertain, particularly for subarctic and Arctic lakes where direct measurements of CH$_4$ and CO$_2$ emissions are often of low temporal resolution and are rarely sustained throughout the entire year.

Using the eddy covariance method, we measured surface–atmosphere exchange of CH$_4$ and CO$_2$ during 2.5 years in a thawed fen and a shallow lake of a subarctic peatland complex. Gas exchange at the fen exhibited the expected seasonality of a subarctic wetland with maximum CH$_4$ emissions and CO$_2$ uptake in summer, as well as low but continuous emissions of CH$_4$ and CO$_2$ throughout the snow-covered winter. The seasonality of lake fluxes differed, with maximum CO$_2$ and CH$_4$ flux rates recorded at spring thaw. During the ice-free seasons, we could identify surface CH$_4$ emissions as mostly ebullition events with a seasonal trend in the magnitude of the release, while a net CO$_2$ flux indicated photosynthetic activity. We found correlations between surface CH$_4$ emissions and surface sediment temperature, as well as between diel CO$_2$ uptake and diel solar input. During spring, the breakdown of thermal stratification following ice thaw triggered the degassing of both CH$_4$ and CO$_2$. This spring burst was observed in 2 consecutive years for both

gases, with a large inter-annual variability in the magnitude of the CH$_4$ degassing.

On the annual scale, spring emissions converted the lake from a small CO$_2$ sink to a CO$_2$ source: 80 % of total annual carbon emissions from the lake were emitted as CO$_2$. The annual total carbon exchange per unit area was highest at the fen, which was an annual sink of carbon with respect to the atmosphere. Continuous respiration during the winter partly counteracted the fen summer sink by accounting for, as both CH$_4$ and CO$_2$, 33 % of annual carbon exchange. Our study shows (1) the importance of overturn periods (spring or fall) for the annual CH$_4$ and CO$_2$ emissions of northern lakes, (2) the significance of lakes as atmospheric carbon sources in subarctic landscapes while fens can be a strong carbon sink, and (3) the potential for ecosystem-scale eddy covariance measurements to improve the understanding of short-term processes driving lake–atmosphere exchange of CH$_4$ and CO$_2$.

1 Introduction

Lakes and wetlands are linked to the atmospheric carbon pool via the exchange of methane (CH$_4$) and carbon dioxide (CO$_2$), which are two important climate-forcing gases (Myhre et al., 2013). While wetlands have been a focus of study due to their high CH$_4$ source function (Christensen et

al., 2003; Crill et al., 1988; Olefeldt et al., 2013) and carbon sequestration capacity (Kayranli et al., 2009; Whiting and Chanton, 2001), lakes have only recently been incorporated together with streams as a separate source into global CH_4 budgets with an uncertain global emission rate of 8–73 Tg CH_4 yr^{-1} (Kirschke et al., 2013). The low number of experimental studies and the variability in the magnitude of emissions across lake types (Wik et al., 2016) explain some of this large uncertainty. Carbon emissions from lakes outweigh part of the land carbon sink, because they emit CH_4 (Bastviken et al., 2011) and because they respire as CO_2 a portion of the carbon that is transported laterally from terrestrial soils to lakes (Algesten et al., 2004; Battin et al., 2009; Cole et al., 2007; Tranvik et al., 2009). Hence, lakes play an important role within the terrestrial carbon budget.

Wetlands and lakes are particularly abundant in the subarctic and boreal regions (Smith et al., 2007; Verpoorter et al., 2014), where climate warming is occurring at a faster pace than in the rest of the world (Serreze and Barry, 2011). In this context, freshwaters have received increasing attention over the past decade, due to the potential for lakes and particularly Arctic thermokarst lakes to exert a feedback on climate warming through large CH_4 emissions (Walter Anthony et al., 2016; Walter et al., 2006). While non-thermokarst, post-glacial lakes emit less CH_4 per unit area (Sepulveda-Jauregui et al., 2015; Wik et al., 2016), they cover a larger area and may as a whole emit half of the total CH_4 emissions (16.5 ± 9.2 Tg CH_4 yr^{-1}) recently attributed to northern (> 50° N) lakes and ponds (Wik et al., 2016).

Biogenic CH_4 production (methanogenesis) occurs in anoxic environments such as lake sediments and water-saturated peat (Cicerone and Oremland, 1988). The process is controlled by the interplay between temperature and the input of organic matter (Kelly and Chynoweth, 1981; Yvon-Durocher et al., 2014; Zeikus and Winfrey, 1976). In lakes and waterlogged wetlands, CH_4 reaches the atmosphere from its production zone via direct bubble release up to the surface (ebullition), through emergent vascular plants, or via turbulence-driven diffusion through the water column (Bastviken et al., 2004; Lai, 2009; Rudd and Hamilton, 1978). The net flux of CH_4 at the lake surface is a balance between the production in the sediments and the oxidation of CH_4 into CO_2 at oxic–anoxic boundaries within the water column (Casper, 1992). In shallow lakes, ebullition is a main pathway for CH_4 to reach the atmosphere while bypassing the oxidation zones (Bastviken et al., 2004). In wetlands, transport from the peat soil to the surface through vascular plants by passive diffusion or by pressurization effects depending on the plant species (Brix et al., 1992) is an efficient pathway for CH_4 to avoid oxidation in the soil and water before reaching the atmosphere (Joabsson and Christensen, 2001).

Dissolved CO_2 in lakes is produced throughout the water column and sediments (Casper et al., 2000) or is directly imported from the catchment (Maberly et al., 2013; Wey-

henmeyer et al., 2015). In situ production comes from the mineralization or the photochemical oxidation of carbon (C) input from the surrounding catchment (Cory et al., 2014; Dillon and Molot, 1997; Duarte and Prairie, 2005) and from the degradation of locally produced organic carbon. CO_2 exchange across the air–water interface is primarily via diffusive release rather than ebullition (e.g., Casper et al., 2000). Lake waters are generally observed to be supersaturated in CO_2 with respect to atmospheric values due to in-lake respiration processes outweighing rates of primary production (Duarte and Prairie, 2005; Sobek et al., 2005). Hence they are generally CO_2 sources to the atmosphere, albeit nutrient-rich lakes and ponds can be small CO_2 sinks during summer months (Huotari et al., 2011) or an entire summer season (Laurion et al., 2010; Pacheco et al., 2013; Shao et al., 2015; Striegl and Michmerhuizen, 1998; Tank et al., 2009).

Near-surface atmospheric forcing is a key driver for the transport and net emissions of gases from a lake to the atmosphere. Ebullition of CH_4 in lakes is partly triggered by water level changes or drops in atmospheric pressure (Casper et al., 2000; Mattson and Likens, 1990), as a decrease in the hydrostatic pressure of the overlying water column on gas saturated sediments favors the release of bubbles (Varadharajan and Hemond, 2012). Wind-driven turbulence is a recognized driver of diffusion-limited exchange of CO_2 and CH_4 across the lake-water interface (Sebacher et al., 1983; Wanninkhof et al., 1985). Convective mixing due to the cooling of the lake surface or following the breakdown of thermal stratification in the water column can increase advection of gas-rich water from the lake bottom, thus enhancing the diffusion-limited release of gases to the atmosphere (Eugster, 2003; MacIntyre et al., 2010; Podgrajsek et al., 2015), especially if the main source of those gases is the sediments, as is the case for CH_4.

Northern ecosystems have strong seasonal contrasts, with short growing seasons and long snow-covered winters. A snow cover insulates the soil from very cold air temperatures (Bubier et al., 2002), while an ice lid on a lake temporarily inhibits the exchanges of gas and heat between the water and the atmosphere (e.g., Greenbank, 1945) and greatly dampens wind-driven turbulence in the water column. In lakes, gases can accumulate at the bottom during long stratification periods, or under lake ice. Lake overturn events most often occur in spring for seasonally ice-covered lakes and/or in fall if lakes thermally stratify during summer (Kirillin et al., 2012; Wetzel, 2001). Overturn events can thus lead to the fast release of accumulated gas to the atmosphere (Jammet et al., 2015; Michmerhuizen et al., 1996; Phelps et al., 1998), but also to the input of atmospheric oxygen, thus increasing the potential for methanotrophy (Kankaala et al., 2006; Schubert et al., 2012). Extension of observations across all seasons of the year is rare at high northern latitudes, particularly for lakes, yet is indispensable for reducing the uncertainty in the magnitude of annual carbon exchange and improving understanding of the processes driving them.

Common methods to measure lake–atmosphere fluxes include floating chambers (e.g., Bastviken et al., 2004), gas transfer models (e.g., Cole and Caraco, 1998), and bubble traps (e.g., Walter et al., 2008; Wik et al., 2013; Sepulveda-Jauregui et al., 2015). If these methods are not integrated and combined, they inherently omit part of the total surface flux. The application of the eddy covariance (EC) method (Aubinet et al., 2012; Moncrieff et al., 1997) to lake environments (e.g., Anderson et al., 1999; Eugster, 2003; Huotari et al., 2011; Mammarella et al., 2015; Podgrajsek et al., 2014; Shao et al., 2015) offers long-term flux monitoring and is a potential methodological solution for solving the spatial and temporal issues of measuring total gas exchange in lakes. Few studies, so far, have used eddy covariance to quantify long-term CO_2 emissions from boreal lakes (Huttunen et al., 2011) as well as CH_4 emissions from boreal (Podgrajsek et al., 2014) or subarctic lakes (Jammet et al., 2015). We report here one of the first year-round eddy covariance measurements of both CH_4 and CO_2 fluxes from a seasonally ice-covered lake.

Surface fluxes were monitored using the eddy covariance method in a subarctic permafrost peatland undergoing thaw, a landscape with a high percentage of pond and lake coverage. The location of the flux tower allowed for measurements to alternate between surface fluxes from a shallow lake and from a permafrost-free, waterlogged fen-type wetland. The overall aim of this work was to quantify year-round carbon fluxes in a post-glacial lake, a type widely present around the subarctic, as compared to the adjacent fen. Specifically, the objectives were (1) to compare the seasonality of CH_4 and CO_2 fluxes from two contrasting subarctic ecosystems (lake and fen), (2) to explore the possibility of identifying short-term environmental controls on the surface–atmosphere exchange of CH_4 and CO_2 in a lake, using high, sub-daily temporal resolution measurements covering all seasons of the year, and (3) to assess and compare the annual atmospheric carbon budget of a lake and a wetland.

2 Materials and methods

2.1 Study site

Stordalen Mire is a subarctic peatland complex (68°20′ N, 19°03′ E) with a high lake and pond coverage, located near Abisko in northern Sweden. Mean annual temperature in the Abisko region has been increasing and fluctuating around 0 °C since the 1990s as part of an accelerated warming trend (Callaghan et al., 2010). Permafrost, which is discontinuously present in the local mires, has been thawing at an increased rate since the 1990s in the peatlands of the region, sometimes disappearing completely (Åkerman and Johansson, 2008). In Stordalen Mire permafrost thawing has led to changes in microtopography, which controls local hydrology, which in turn leads to vegetation shifts (Chris-
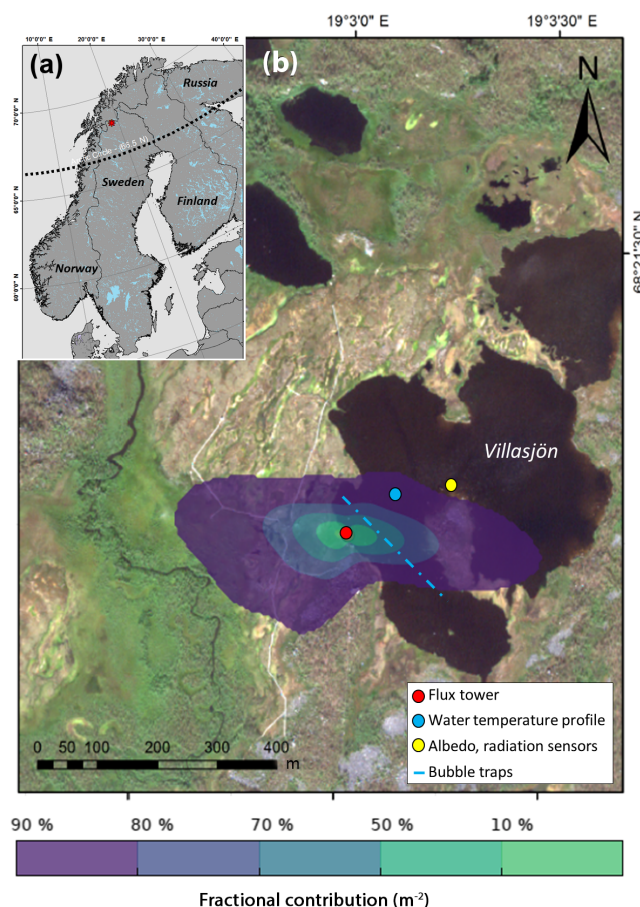

Figure 1. Location of the study site **(a)** and flux footprint of the flux tower in summer averaged over all years **(b)**. The color scale indicates the extent of the fractional contribution from the source area to the fluxes measured at the tower. The location of the flux tower is indicated along with the location of the main environmental data sources.

tensen, 2004; Malmer et al., 2005). This accentuates the heterogeneity of a landscape comprised of elevated palsas with permafrost, thawing lawns with thermokarst ponds, and permafrost-free, water-saturated fens. The mire is bordered by post-glacial lakes on its western, northern, and eastern edges. This study focuses on the lake Villasjön (Fig. 1) and the adjacent fen to the west of the tower. According to Olefeldt and Roulet (2012), the two ecosystems are hydrologically connected with a directional flow from the lake to the fen.

The wetter fen areas have expanded as a result of permafrost thaw over the past decades (Johansson et al., 2006). The water table of the fen is at or above the surface throughout the year. The dominant vegetation species are vascular plants *Carex rostrata* and *Eriophorium angustifolium*. Villasjön is the largest (0.17 km^2) lake of the 15 km^2 wide Stordalen catchment containing 27 lakes (Lundin et al., 2013). It has mean and maximum depths of 0.7 and 1.3 m,

respectively (Jackowicz-Korczyński et al., 2010; Wik et al., 2013). The upstream catchment of Villasjön is dominated by birch forest (Olefeldt and Roulet, 2012), while its western shore is bordered by thawing palsas. During snowmelt, there is a small surface inflow feeding Villasjön in the east (Wik et al., 2013). The lake usually freezes to the bottom in winter. The DOC concentration in the lake water was measured to be 8.1 mg L^{-1} in 2008 (Olefeldt and Roulet, 2012). Aquatic vegetation is present in the lake, on its bottom as algae, as submerged plants within its southern arm, and in a low density of emergent macrophytes at its shores.

2.2 Eddy covariance measurements

2.2.1 Measurement setup

Between June 2012 and December 2014, the surface–atmosphere exchange of CH$_4$, CO$_2$, and latent heat and sensible heat was monitored nearly continuously with an eddy covariance setup located at the shore of Villasjön (Fig. 1). Data were logged on a CR1000 (Campbell Scientific, Inc., UT, USA) until May 2013; from June 2013 it was replaced with a CR3000 (Campbell Scientific, Inc., UT, USA). The 2.92 m high mast was equipped with a 3-D sonic anemometer (R3-50, Gill Instruments Ltd.) sampling wind components and sonic temperature at 10 Hz. Throughout the study period, ambient molar densities of CO$_2$ and H$_2$O were sampled at 10 Hz with an open path infrared gas analyzer (IRGA), model LI7500 (LICOR Environment, NE, USA), mounted on the mast at 2.50 m height. Following lightning that hit the electric grid in Stordalen Mire on 27 July 2013, the initial LI7500 ceased functioning and was replaced on 1 October 2013 by a different instrument of the same model.

From June 2012 to May 2013, the ambient CH$_4$ mole fraction was sampled at 10 Hz with a closed path Fast Greenhouse Gas Analyzer (FGGA, Los Gatos Research, CA, USA) in air that was taken from a gas inlet located at 2.50 m height on the mast through a 6 mm inner diameter polyethylene (PE) tube using a dry scroll pump (Varian TriScroll 300). The efficient flow rate in the 95 m long sampling line was 16 L min^{-1}, ensuring the maintenance of turbulent conditions (Reynolds number ca. 4025). On 5 June 2013, the tube was replaced with an 8 mm inner diameter PE tube, which changed the flow rate in the sampling line to 23.88 L min^{-1} (Reynolds number ca. 4099). On 4 August 2013, the closed path CH$_4$ system was renewed: the IRGA was changed to a FGGA model 911-010 (Los Gatos Research, CA, USA). Due to instrumental maintenance, the IRGA was offline between February and March 2014 and replaced on 24 March 2014 by the previous FGGA. From August 2013 to December 2014, due to a failure in the electronic connection between the gas analyzer and the data logger, the raw CH$_4$ data measured by the FGGA were pre-processed in order to align the time stamp and frequency of the gas analyzer recordings with the time stamp of the logger sampling the wind data. The synchronization procedure was quality-checked after flux computation (Supplement S2). Each change in the CH$_4$ measurement setup was taken into account in the flux calculation.

2.2.2 Flux calculation and quality check

CO$_2$, CH$_4$, sensible and latent heat fluxes, as well as atmospheric turbulence quantities were calculated and output as 30 min averages using the EddyPro version 5.2 open-source software (hosted by LICOR Environment, USA). Processing of the 10 Hz raw data followed standard eddy covariance procedures (Aubinet et al., 2012; Lee et al., 2005); methodological choices differed partly for CH$_4$ and CO$_2$ flux processing, as detailed in Appendix A.

The 30 min averaged fluxes were quality-checked to detect measurement errors and to ensure the fulfillment of theoretical assumptions for the application of the eddy covariance method. Spikes were present in the CO$_2$ flux time series, which can be due to weather conditions, fast changes in the atmosphere's turbulent conditions, or faulty instrumentation. Outliers in the CO$_2$ flux dataset were detected using the median of absolute deviation from the median (MAD) as described in Papale et al. (2006) using a threshold $z = 4$ and with no distinction between day and night. Additionally, CO$_2$ flux averaging periods were rejected when the number of spikes per half hour was > 100 (Mammarella et al., 2015) and when skewness and kurtosis were outside the $[-2,2]$ and $[1,8]$ ranges (Vickers and Mahrt, 1997), respectively. Required flux stationarity (FST) within the 30 min flux averaging period was ensured by rejecting each flux value when the FST criterion as defined by Foken and Wichura (1996) was above 0.3, a strict criterion that was chosen, given the challenging footprint on the lake side, to ensure that fluxes represented the surface of interest. The fen part of the CO$_2$ flux dataset was additionally filtered for poorly developed turbulence (Mauder and Foken, 2006) and u^*-filtered (Papale et al., 2006) with a threshold determined to be 0.1 m s^{-1} using the online tool available at https://www.bgc-jena.mpg.de/bgi/index.php/Services/REddyProcWeb (Reichstein et al., 2005). The impact of self-heating on the open path CO$_2$ flux measurements (Burba et al., 2008) is a potential issue when using the LI7500 model, especially for low-flux environments. It could not be correctly quantified in this study and was thus not applied to avoid a potentially large systematic error. A rough estimate of the correction indicated that it could increase the magnitude of the CO$_2$ fluxes by 0.28 µmol m^{-2} s^{-1} on average.

Quality check and screening of the CH$_4$ flux time series included rejection of averaging periods when the number of spikes per half hour was > 100. Fluxes were rejected when skewness and kurtosis were outside the pre-cited range, in winter only, due to the pulse character of CH$_4$ emissions during non-winter periods that could be misinterpreted as faulty raw data due to a high skewness (Jammet et al., 2015). Flux stationarity within the averaging time period was also en-

sured by rejecting values when the FST criterion was above 0.3. Additionally, flux values for which a time lag was not found within the plausibility time lag window were rejected (Eugster et al., 2011; Wille et al., 2008). Gaps were initially present in the flux dataset due to instrument malfunctioning, particularly in winter, and power cuts (Fig. S6 in the Supplement). After quality check and filtering, in total 13 474 CH$_4$ fluxes and 11 629 CO$_2$ fluxes were available for further analysis (Table S1, Fig. S6 in the Supplement). The data rejection rate was high; eddy covariance studies in lake environments usually report high rejection rates from quality-check routines (Jonsson et al., 2008; Mammarella et al., 2015; Nordbo et al., 2011).

2.3 Flux footprint and partitioning between lake and wetland

As in Jammet et al. (2015), the bidirectional wind pattern at the Stordalen Mire was used to partition the flux dataset into two main wind sectors which crossed the two different studied ecosystems. To ensure a clear distinction between the lake and the fen fluxes and the homogeneity of each surface, the lake sector was conservatively defined as 20–135°, and the fen sector as 210–330° (0° = 360° is true north). Over the study period, 46.2 % of the measured fluxes originated from the lake sector, 45.7 % of the measured fluxes originated from the fen sector, and the residual 8.1 % of the measured flux data was excluded, for being of lower wind speed and originating from mixed sources. Each season was nevertheless well represented in the flux dataset of each ecosystem (fen and lake) thanks to regular shifts in wind direction.

The flux footprint was calculated using a 2-D model developed by Kljun et al. (2015). Inputs to the model include turbulence quantities measured at the tower (friction velocity (u^*), standard deviation of cross-wind velocity (σ_v), Obukhov length, horizontal wind speed), height of the boundary layer (derived from the Era-Interim reanalysis product; Dee et al., 2011), the measurement height and the surface roughness length which was separately estimated for the lake (0.001 m), and the fen sectors (0.002 m in winter to a maximum of 0.10 m in summer, accounting for vegetation growth). Footprints were calculated for each 30 min time step where the required data were available, and averaged for the periods of interest (summer and winter).

According to the footprint model, most of the flux measured at the tower (peak fetch) originated from a distance of 38 m on the fen sector and 73 m on the lake sector, on average during the ice-free season. The lake surface was within the cumulative 80 % of flux footprint during the ice-free seasons (Fig. 1). In winter, the footprint model revealed that the 80 % cumulative footprint, on the lake side, included part of the land in the middle of the lake (Fig. S1 in the Supplement). This is likely due to the lower roughness length (snow cover), but also to more stable atmospheric conditions: the sensible heat flux H is negative during most of the winter

and the atmospheric stability parameter indicated more stable conditions in winter as compared to summer conditions. Thus, to avoid large contamination of the land respiration in the winter lake fluxes due to an extended footprint over the lake shores, the winter fluxes from the lake sector were only kept for further analysis when the standard deviation of lateral wind velocity $\sigma_v \leq 1\,\mathrm{m\,s^{-1}}$ (Forbrich et al., 2011) in order to limit lateral contamination of CO$_2$ fluxes into the footprint area of interest. This removed an additional 3.7 % of the lake CO$_2$ flux dataset.

2.4 Ancillary measurements

Supporting environmental variables were measured at 1 Hz and averaged and logged every half hour. Temperature probes (T107, Campbell Scientific, Inc., UT, USA) were installed in the peat 5 m south-west of the tower at 5, 10, 25, and 50 cm depths. Net radiation at the fen surface was recorded with an REBS Net Radiometer, model Q7.1 (Campbell Scientific, Inc., UT, USA). Air temperature used in this study was measured at 2 m height on a mast located in the middle of the lake (Fig. 1) with a CS215 probe (Campbell Scientific, Inc., UT, USA). At the same mast, radiation components were measured with a CNR4 Net Radiometer (Kipp & Zonen, the Netherlands) from which net radiation at the lake surface was computed. Water temperature in the center of the lake (Fig. 1) was measured at 10, 30, 50, and 100 cm depths with inter-calibrated HOBO Water Temp Pro v2 loggers (Onset Computer Corporation, MA, USA). The loggers are suspended on a nylon line from a mooring float, which stays at the surface throughout the year. The string assembly was designed so that the bottom sensor at 100 cm depth is in the surface sediment. Lake surface albedo was computed daily as the midday ratio (10:00 to 13:00 UTC+1) of the shortwave radiation components, and used in combination with temperature data to delimit the ice-cover seasons. Air pressure and precipitation were measured at a weather station 640 m south of the eddy covariance mast.

2.5 Gap filling of CH$_4$ and CO$_2$ flux time series

The estimation of annual carbon exchange budgets required filling of the gaps in the CH$_4$ and CO$_2$ flux time series. When working with highly skewed flux datasets such as CH$_4$ emissions from lakes (Fig. C1), integrating the mean flux over the whole time period may lead to important overestimation. There is as yet no published account of gap filling CH$_4$ fluxes measured with eddy covariance. In the present study, gap filling of the CH$_4$ flux time series was performed separately on the lake and fen flux datasets, using artificial neural networks (ANNs) (Moffat et al., 2010; Papale and Valentini, 2003). ANNs are multivariate, nonlinear regression models that are fully empirical: the observational data are used to constrain the model's numerical relationship between the inputs (independent variables, i.e., environmental drivers) and outputs

(dependent variables, i.e., fluxes) (Moffat et al., 2010). ANNs have been tested and successfully used to estimate missing values and gap fill CO$_2$ flux time series measured with eddy covariance in forests (Moffat et al., 2007; Papale and Valentini, 2003) or in urban terrain (Järvi et al., 2012) and to gap fill CH$_4$ emissions in wetlands (Dengel et al., 2013). To our knowledge, we present the first attempt at using ANNs to gap fill eddy covariance measurements of CH$_4$ emissions from a lake.

Three ANN models were built separately on CH$_4$ emissions from the fen, CH$_4$ emissions from the lake, and CO$_2$ emissions from the fen, on the hourly scale. Model development followed workflows introduced by Papale and Valentini (2003), Moffat et al. (2007), and Dengel et al. (2013). Environmental variables to be included as inputs were selected according to their physiological relevance to the production and transport of CH$_4$ and CO$_2$ from the surface to the atmosphere, as reported in the literature. The relevance of the drivers was confirmed by correlation analysis. Input variables used for each model are reported in Table B1. A further detailed description of ANN model development can be found in Supplement S1. Gaps in the measured CH$_4$ and CO$_2$ flux time series were replaced by predicted values, and the annual sums were computed by integrating the hourly flux values over time. The performance of the ANN models was assessed by comparing the predicted values with original observed values over the whole dataset (Appendix B).

The ANN method did not perform well on the lake CO$_2$ flux time series, which comprised a large number of gaps and a high signal-to-noise ratio. ANN results were thus excluded for the lake CO$_2$ fluxes to avoid introducing a high and unnecessary uncertainty. Instead, the seasonal lake CO$_2$ exchange was computed by multiplying the mean flux rate during each season by the number of days. Considering the normal distribution of the CO$_2$ lake fluxes (Fig. C1), this method was considered an acceptable way of filling missing values.

2.6 Uncertainty analysis

The total random error is a composite of errors associated with instrument noise, the stochastic nature of turbulence, the instrument precision, and the variation of the flux footprint (Moncrieff et al., 1996). The relative random error increases with the magnitude of the flux (Richardson et al., 2006), while over time it decreases with increasing size of the dataset because of its random nature (Moncrieff et al., 1996). It is therefore negligible when propagated over annual sums, but can be important for single flux values. The random error was calculated as the sampling error for each flux value in the flux calculation software using the method of Finkelstein and Sims (2001).

The mean random error of the quality-checked measured CH$_4$ fluxes was 2.9 ± 4.3 (mean $\pm$ SD) nmol m^{-2} s^{-1} at the lake and 4.7 ± 3.8 nmol m^{-2} s^{-1} at the fen, which

corresponds to 7.6 and 6 % of the overall mean measured fluxes, respectively. This is in the lower end of ranges reported for CO$_2$ and energy fluxes. The mean random error of the individual measured lake CH$_4$ fluxes was highest in winter (24 %) and lowest during the thaw season (11 %) when the largest fluxes were measured. The mean random error of the quality-checked measured CO$_2$ fluxes was 0.20 ± 0.57 µmol m^{-2} s^{-1} at the lake and 0.32 ± 0.48 µmol m^{-2} s^{-1} at the fen, equivalent to 31 and 13 %, respectively, of the overall mean absolute measured flux, indicating that our setup was able to measure both CH$_4$ and CO$_2$ fluxes observable at our site. These values are comparable to what has been reported in vegetated (Finkelstein and Sims, 2001), urban (Järvi et al., 2012), boreal lake (Mammarella et al., 2015), and other typical eddy covariance sites (Rannik et al., 2016). In spring the random error of CO$_2$ fluxes at the lake was 18 % of the measured flux; however, during the ice-free season it was above the absolute measured flux in 20 % of the cases. Thus air–lake CO$_2$ exchange rates during the summer were low and sometimes close to the detection limit.

The random error of the fluxes modeled with ANN (Appendix B) was on average 4 nmol m^{-2} s^{-1} for fen CH$_4$ fluxes, 0.23 µmol m^{-2} s^{-1} for fen CO$_2$ fluxes, and 11 nmol m^{-2} s^{-1} for lake CH$_4$ fluxes. These errors were small when propagated onto seasonal and annual sums using the random error propagation principle (Moncrieff et al., 1996). The systematic bias in the annual flux due to the gap filling method, the bias error (BE), was calculated on the seasonal and annual flux sums as in Moffat et al. (2007) as the sum of the difference between the predicted values p_i and the observed values o_i:

$$\text{BE} = \frac{1}{N} \sum (p_i - o_i), \tag{1}$$

where N is the number of gap filled values in the flux time series. The bias error adds up over time. It was multiplied by the number of gap filled values to obtain a total seasonal and annual offset (Moffat et al., 2007). The offset can be the largest source of uncertainty in the computation of annual budgets. The systematic offset due to gap filling was larger for annual CO$_2$ fen fluxes (Table 3), likely because of the higher noise in the measurements and higher number of gaps during the second year. For total lake CO$_2$ fluxes, the annual BE was calculated in the same way, using the seasonal mean as the predicted values. The resulting offset due to gap filling was close to zero (Table 3), because flux values were normally distributed, which confirms that using the mean did not induce a significant bias for this particular dataset.

2.7 Definition of seasons

Observations started in June 2012 and were sustained nearly continuously until December 2014. We adopted a lake-centric definition of seasons based on the lake ice phenol-
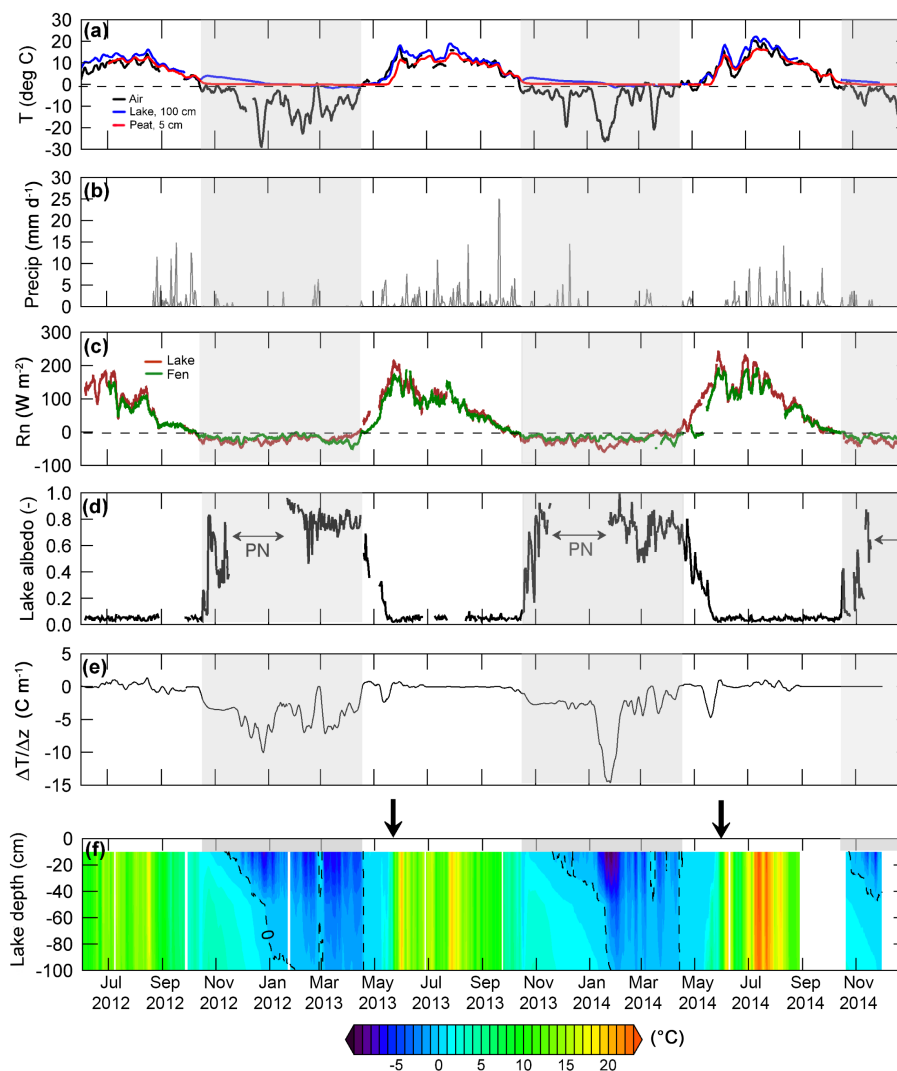
Figure 2. Daily mean of air, peat, and surface sediment temperature **(a)**; cumulative daily precipitation **(b)**; daily mean net radiation input at the fen and the lake surfaces **(c)**; albedo of the lake surface **(d)**; daily temperature gradient in the lake water column defined as ($T_{w, 10\,cm}$ − $T_{w, 100\,cm}$) divided by the depth difference Δz **(e)**; water temperature profile in the lake center derived from continuous daily temperature measurements at depths 10 cm, 30 cm, 50 cm, and 100 cm (= bottom) **(f)**. The shaded areas indicate the periods of ice cover at the lake. PN stands for polar night, i.e., near zero solar input. The black arrows indicate the estimated time of complete lake overturn after ice-out.

ogy. A full year was defined from 1 June to 31 May of the next year, so that an entire ice-cover season was included in a given year. This keeps the connected thaw period and previous ice-cover season within the same year. The year was further divided into an ice-cover season (winter), an ice-free season (summer and fall), and a thaw season (spring). The thaw season represents a transitional period during which the snow cover and lake ice melt. It is separated from summer, since the hydrological and biogeochemical dynamics in seasonally ice-covered lakes differ from the rest of the open-water season.

Daily air temperature was used to define seasons. The start of the ice-cover season was defined as the start of the lake freeze-up, i.e., the first day on which daily mean air temper-

ature is below zero for 3 consecutive days. Further, this date coincided each year (2012 to 2014) with the formation of thermal stratification in the water column (Fig. 2d) due to a rise in bottom water temperature right after the first day of freezing (Fig. 2a, blue line). This indicates the inhibition of direct heat exchange between the lake and the atmosphere when ice forms at the lake surface. In the first year (2012), the first day of the ice-cover season was confirmed by visual observation of ice over the whole lake surface, while in the following years, these combined temperature observations were used to define the start of ice cover.

The end of the ice-cover season was defined as the start of thaw, i.e., the first date on which daily mean air temperature rose above 0 °C for at least 3 consecutive days. This date

Table 1. Climatic conditions per season: mean air temperature measured at the Abisko Scientific Research Station, peat temperature at 10 cm depth in the fen, surface sediment temperature in the lake (1 m depth), and total incoming solar radiation (S_i). Season delimitations (see text for a definition) are reported for each year.

Season	Year	Dates	Length (days)	Air T (°C)	Peat T at 10 cm (°C)	Surf. sed. T (°C)	Total S_i (10^3 Wm^{-2})
Ice-free	2012	1 June–14 Oct.	136	7.8	8.9	10.2	808
	2013	26 May–15 Oct	143	10.2	9.9	12.0	902
	2014	2 Jun–9 Oct	130	10.4	10.5	12.8	1019
Ice-cover	2012–2013	15 Oct–14 Apr	182	−7.9	0.0	0.7	279
	2013–2014	16 Oct–10 Apr	177	−6.5	0.2	0.8	239
Thaw	2013	15 Apr–25 May	41	4.3	0.3	1.9	250
	2014	11 Apr–1 Jun	52	2.2	1	1.9	502
Annual	2012–2013	1 Jun–31 May	365	−0.3	3.5	4.7	1424
	2013–2014	1 Jun–31 May	365	0.9	4	5.1	1543

preceded by 1 to 2 days the temperature rise to 0 °C in the surface (10 cm) of the lake ice. Further, the start of the thaw season could be confirmed by the increase in mean daily net radiation to net positive values at the lake and the fen surfaces (Fig. 2c) and by a decrease in lake albedo (Fig. 2d) until open-water values were reached (mean = 0.05). We thereby defined two complete ice-cover seasons during the study period: from 15 October 2012 to 14 April 2013 (182 days) and from 16 October 2013 to 10 April 2014 (177 days). In 2014, freeze-up of the lake occurred on 10 October. The ice-cover seasons were systematically characterized by negative daily energy input at the lake and at the fen (Fig. 2). Thus our season definition based on daily air temperature was robust and reproducible each year.

The end of spring (i.e., the thaw season) and the beginning of the ice-free season were defined as the first date with a daily temperature gradient in the water column close to 0 °C m^{-1} after the spring overturn, i.e., when the lake enters its isothermal conditions after complete ice thaw. The dataset of this study covers 2 complete years plus an additional ice-free season, i.e., three ice-free seasons, two ice-cover seasons, and two thaw seasons. Season dates and lengths are summarized in Table 1.

3 Results

3.1 Environmental conditions and lake climatology

Mean annual (June to May) air temperature measured at the Abisko Scientific Research Station was −0.3 °C in 2012–2013 and 0.9 °C in 2013–2014. The latter was significantly above the long-term average (1913–2014) of −0.5 ± 1 °C (mean ± SD). The ice-free season was warmest in 2014 and coolest in 2012 (Table 1). This difference between years was reflected in both the mean daily peat temperature measured at 10 cm depth and the mean daily lake water temperatures,

which were warmest in 2014 (Fig. 2; Table 1). The mean air temperature observed over our study period correlated with total incoming solar radiation, both annually and during the ice-free periods (Table 1). Winter 2013–2014 was on average 2.1 °C warmer than the previous one and the ice-cover season was 5 days shorter due to an earlier thaw start. The thaw period started earlier in 2014 but lasted longer (Fig. 2d, Table 1); complete lake overturn (isothermal water column) following ice thaw occurred 7 days later than in 2013.

The development pattern of thermal stratification along lake depth at freeze-up and its breakdown in spring was similar in both years (Fig. 2d). In both spring 2013 and 2014, the lake overturn occurred after the development of strong thermal stratification in the lake during thaw (Fig. 2e, f). The temperature at the bottom of the lake was up to 4 °C warmer than the surface in spring 2013 and up to 6 °C warmer in 2014, likely indicating the penetration of solar radiation through thinning ice before complete ice-out and full water mixing. The thermal structure at the beginning of freeze-up, as well as during the period of ice thaw preceding spring overturn in 2013, has been previously described in detail for this site in a winter-focused study (Jammet et al., 2015).

During the ice-free, summer season, there was slight to no thermal stratification in the water column (Fig. 2d). The shallow lake water column reacted quickly to temperature changes (Fig. 2a, d) and the dark bottom warmed up quickly since solar radiation can reach the sediment surface. Thus, the lake had a polymictic behavior; i.e., it was regularly mixing to the bottom during the ice-free season, which ensures isothermal conditions in the water column throughout the summer. Water temperature reached a maximum of 23.8 °C in July 2014. Conversely, a strong temperature gradient formed during winter (Fig. 2f). In both winters the surface sediment temperature dropped below 0 °C by February, with minima of −1.9 °C in March 2013 and −1.6 °C in February 2014. This suggests that the water column froze to the

bottom. The temperatures in the peat soil and at the surface sediment in the lake were de-coupled from air temperature (Fig. 2a), showing the hindrance of heat exchange with the atmosphere due to the presence of ice and snow at the surface.

3.2 Year-round CH$_4$ and CO$_2$ fluxes

CH$_4$ emissions from the lake showed a highly skewed distribution (Fig. C1a); there was a large difference between the overall mean ($40\,\mathrm{nmol\,m^{-2}\,s^{-1}}$) and overall median ($12\,\mathrm{nmol\,m^{-2}\,s^{-1}}$). The seasonal flux pattern was characterized by low background emissions and occasional, large degassing events (Fig. 3) with 25 % of measured data above $111\,\mathrm{nmol\,m^{-2}\,s^{-1}}$ in the thaw period, and 5 % of measured data above $75\,\mathrm{nmol\,m^{-2}\,s^{-1}}$ within the ice-free season (Fig. 4). Over the full measurement period, summer emission rates averaged to $26\,\mathrm{nmol\,m^{-2}\,s^{-1}}$ (median $12\,\mathrm{nmol\,m^{-2}\,s^{-1}}$), spring emission rates to $84\,\mathrm{nmol\,m^{-2}\,s^{-1}}$ (median $33\,\mathrm{nmol\,m^{-2}\,s^{-1}}$), and winter emissions to $2.8\,\mathrm{nmol\,m^{-2}\,s^{-1}}$ (median $3.0\,\mathrm{nmol\,m^{-2}\,s^{-1}}$). The mean and median of the winter emissions were not significantly different from the mean random error of the fluxes. CO$_2$ fluxes were close to normally distributed at the lake (Fig. C1b) and the overall mean rate was $0.22\,\mathrm{\mu mol\,CO_2\,m^{-2}\,s^{-1}}$ (median $0.18\,\mathrm{\mu mol\,m^{-2}\,s^{-1}}$). There was a distinctive CO$_2$ outgassing at the time of water overturn during the spring of both 2013 and 2014 (Fig. 3d). The mean measured CO$_2$ exchange at the lake was significantly negative during the ice-free seasons (one sample t-test, $p < 0.001$), $-0.14\,\mathrm{\mu mol\,m^{-2}\,s^{-1}}$, indicating a low net uptake of CO$_2$ (Fig. 4). Negative flux rates started right after the spring CO$_2$ outgassing in 2013 and 2014 (Fig. 3d). The highest CO$_2$ uptake rates were observed during the summer of 2014, which was the warmest summer of the study period, with the highest solar radiation input (Table 1). In fall 2014, a burst of CO$_2$ was measured at the lake, which was not present in previous years (Fig. 3d). This fall burst was not observed in the CH$_4$ flux measurements. Wintertime CO$_2$ emissions from the lake were significantly above the flux random error and significantly positive (Figs. 3d, 4). There was an inter-annual variability in the magnitude of the CH$_4$ spring degassing from the lake between the 2 years (Fig. 3c). In contrast, mean CO$_2$ degassing was higher during the second thaw season, $0.78\,\mathrm{\mu mol\,CO_2\,m^{-2}\,s^{-1}}$ (median $0.47\,\mathrm{\mu mol\,CO_2\,m^{-2}\,s^{-1}}$) in 2013 and $0.99\,\mathrm{\mu mol\,CO_2\,m^{-2}\,s^{-1}}$ (median $0.75\,\mathrm{\mu mol\,CO_2\,m^{-2}\,s^{-1}}$) in 2014. Both CH$_4$ and CO$_2$ emissions during spring were significantly higher than during the following ice-free season, in both years (Fig. S2 in the Supplement).

The distribution of CH$_4$ emissions from the fen was less skewed (Fig. C1a) and the overall measured mean was $77\,\mathrm{nmol\,m^{-2}\,s^{-1}}$ (median $58\,\mathrm{nmol\,m^{-2}\,s^{-1}}$). The highest CH$_4$ emissions at the fen occurred during the ice-free season (Fig. 3), with a mean rate of $110\,\mathrm{nmol\,m^{-2}\,s^{-1}}$

(median $108\,\mathrm{nmol\,m^{-2}\,s^{-1}}$). Sustained CH$_4$ emissions were measured at the fen throughout the winter (Fig. 3), with a mean rate of $25\,\mathrm{nmol\,m^{-2}\,s^{-1}}$ (median $25\,\mathrm{nmol\,m^{-2}\,s^{-1}}$). Flux rates during the snowmelt and thaw season averaged to $35\,\mathrm{nmol\,m^{-2}\,s^{-1}}$ (median $33\,\mathrm{nmol\,m^{-2}\,s^{-1}}$). CO$_2$ fluxes from the fen averaged to $-1.3\,\mathrm{\mu mol\,m^{-2}\,s^{-1}}$ (median $0.2\,\mathrm{\mu mol\,m^{-2}\,s^{-1}}$) over the full period, and the mean rate was $-2.6\,\mathrm{\mu mol\,m^{-2}\,s^{-1}}$ during the ice-free seasons. CO$_2$ respiration was sustained throughout winter (Fig. 3b) at a mean rate of $0.8\,\mathrm{\mu mol\,m^{-2}\,s^{-1}}$, and the release of CO$_2$ during the melt season was low (Fig. 4).

The average annual seasonality of CH$_4$ and CO$_2$ fluxes in both ecosystems is shown in Fig. 5. The lake dominated CH$_4$ and CO$_2$ emissions during spring. During the ice-free seasons, by contrast, the lake was a lower emitter of CH$_4$ than the fen per unit area, and its CO$_2$ exchange was close to neutral with a small uptake. There was a slight seasonality in CH$_4$ lake emissions during summer but, annually, CH$_4$ and CO$_2$ lake fluxes peaked in spring (Fig. 5). CH$_4$ emissions from the fen peaked in August and net CO$_2$ exchange peaked in July (Fig. 5). The emission of both gases occurred at lower rates but continuously in winter.

3.3 Variability of lake–air carbon exchange within seasons

The thaw and ice-free periods are different in terms of flux dynamics. The dataset was therefore separated into seasons to explore controls on the lake fluxes. During the ice-free seasons, half-hourly CH$_4$ fluxes at the lake were characterized by degassing events that coincided with drops in atmospheric pressure (Fig. 6). Daily EC flux data were compared with spatially averaged, daily ebullition fluxes measured in the lake with ebullition traps located nearby or within the tower footprint. The degassing events measured with the eddy covariance system coincided in timing and in magnitude with the daily ebullition fluxes measured with the ebullition traps (Fig. 6).

Due to the high skewness of the CH$_4$ lake flux dataset (Fig. C1) and the presence of outliers in both CO$_2$ and CH$_4$ flux datasets from the lake, we used Spearman's ρ coefficient, which is a statistical measure of association that is robust to outliers and applicable to skewed distribution (Kowalski, 1972), to explore bivariate associations. Among potential flux drivers, the highest correlation of ice-free CH$_4$ emissions was found with surface sediment temperature ($\rho = 0.49$, Table 2). Degassing events occurred often after an increase in surface sediment temperature (Fig. 6). When averaging all 30 min CH$_4$ fluxes during the three ice-free seasons per bins of $1\,^\circ\mathrm{C}$, an exponential regression between lake CH$_4$ fluxes and surface sediment temperature could explain 82 % of the variability in CH$_4$ emissions (Fig. 7).

Wind speed correlated best with CH$_4$ lake emissions during the thaw period (Table 2, $\rho = 0.40$). The relationship was weaker during the open-water period. We observed a

Table 2. Statistical exploration of the lake flux dataset: Spearman's rank correlation coefficient (ρ) shows the degree of association between half-hourly lake CH_4 flux and lake CO_2 flux with potential drivers of variability. All data were grouped per season. See Table 1 for the limitation of the seasons. Lake fluxes are filtered in winter for high standard deviation of lateral wind speed.

	Lake CH_4 flux (Spearman's ρ)				Lake CO_2 flux (Spearman's ρ)			
	Annual	Ice-free	Thaw	Ice-cover	Annual	Ice-free	Thaw	Ice-cover
Air T	0.36***	0.40***	0.26***	0.14**	−0.21***	−0.22***	0.38***	0.16***
T water surface	0.27***	0.48***	0.37***	0.18*	−0.21***	−0.21***	0.27***	0.09***
T bottom	0.24***	0.49***	0.49***	0.10*	−0.26***	−0.21***	0.40***	−0.10***
Wind speed	0.36***	0.32***	0.40***	0.27***	0.26***	0.13***	0.38***	0.36***
H flux	−0.15***	0.12***	−0.18***	−0.12*	−0.62***	−0.67***	−0.38***	−0.50***
LE flux	0.24***	0.38***	0.16***	0.08	-0.29***	-0.49***	0.05	−0.14***
Solar radiation	0.27***	0.13***	−0.02	−0.11*	−0.09***	−0.52***	0.02	−0.22***
CO_2 flux	0.41***	−0.13***	0.67***	0.21**	–	–	–	–

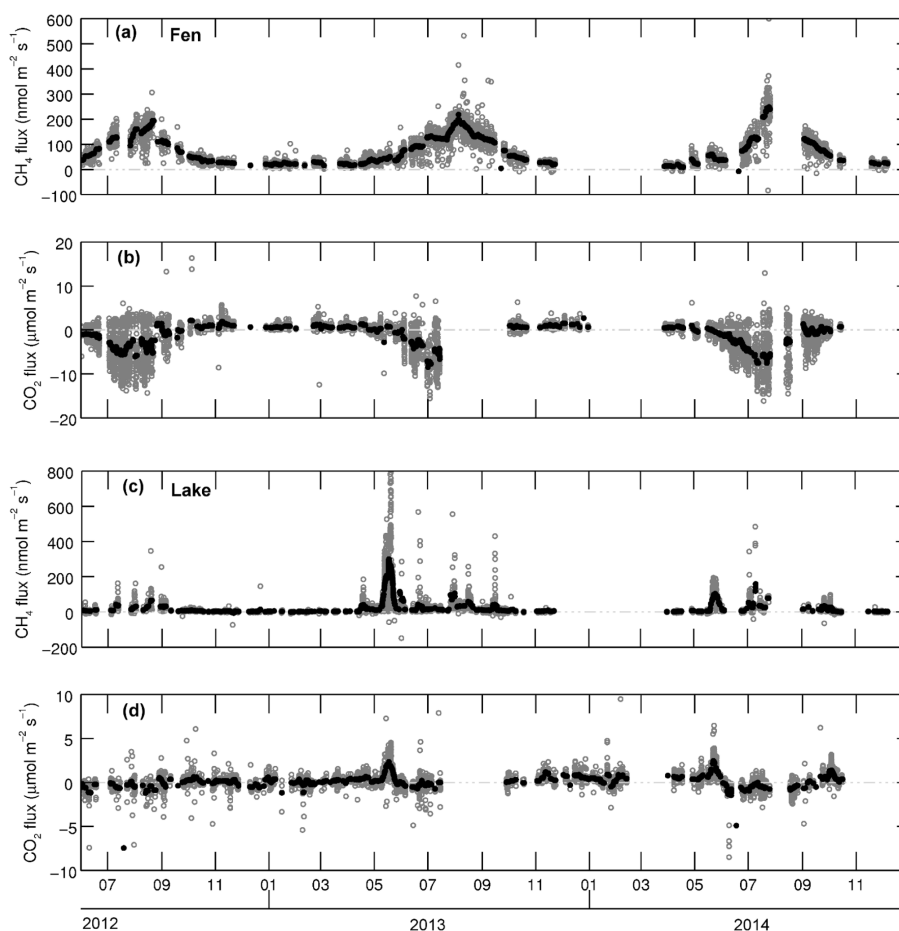* p-value < 0.1; ** p-value < 0.01; *** p-value < 0.001.

Figure 3. Measured CH_4 and CO_2 fluxes at the fen **(a, b)** and the lake **(c, d)** over the full study period. Light grey dots are half-hourly values and black dots show a 5-day running mean. Note on panel **(c)**: nine flux values above $800\,\mathrm{nmol\,m^{-2}\,s^{-1}}$ are not displayed for visibility.

few CH_4 degassing events in summer that coincided with the likely mixing of the water column following a short period of thermal stratification (0.8 to 1 °C gradient between 10 and 100 cm depths, Fig. S3a, b in the Supplement), but

these were not systematic (Fig. S3c, d in the Supplement). During the ice-free season, there was a weak anti-correlation between CO_2 exchange at the lake and air and water temperature (Table 2). Wind speed correlated weakly with CO_2

Table 3. Seasonal and annual sums of CO$_2$ and CH$_4$ fluxes after gap filling, in g C m^{-2} yr^{-1}. Sum BE is the bias due to the gap filling model (Eq. 1), scaled to annual flux units and multiplied by the number of gaps in the flux dataset over the season or year. The sum of CO$_2$ fluxes from the lake is only reported for the first year.

Season	Year	Fen CH$_4$ flux		Lake CH$_4$ flux		Fen CO$_2$ flux		Lake CO$_2$ flux	
		Total flux	Sum BE	Total flux	Sum BE	Total flux	Sum BE	Total flux	Sum BE
Ice-free	2012	14.8	0.1	2.5	−0.1	−179.4	−14.8	−24.4	< 0.001
	2013	16.2	−0.1	2.8	−0.1	−201.3	13.2	nc*	nc
	2014	16.8	0.09	3.0	−0.5	−239.6	−5.1	nc	nc
Ice-cover	2012–2013	4.1	−0.2	0.3	−0.3	109.6	−8.8	12.4	< 0.001
	2013–2014	4.2	0.7	0.4	−0.4	115.5	20.7	nc	nc
Thaw	2013	1.4	−0.1	2.5	−0.2	11.3	−0.4	33.3	< 0.001
	2014	1.7	−0.07	1.3	0.5	11.7	1.1	nc	nc
Annual	2012–2013	20.3	0.2	5.3	−1.9	−58.5	−26.1	21.5	< 0.001
	2013–2014	22.1	−0.1	4.4	0.6	−74.1	97.4	nc	nc
Annual	Average ± SD	21.2 ± 1.3	−0.2	4.9 ± 0.6	−0.7	−66.3 ± 11	35.7	21.5	< 0.001

* nc: not computed.
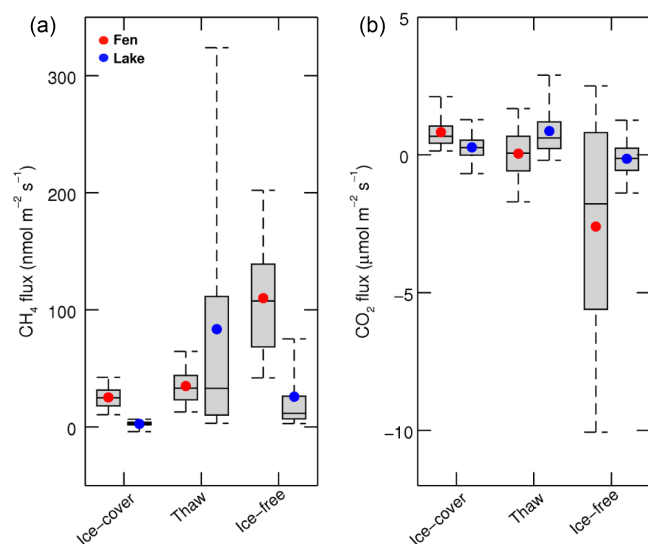
Figure 4. Measured flux rates of CH$_4$ **(a)** and CO$_2$ **(b)** per season and per ecosystem. The central line of the boxplots shows the median, box edges show the 25th and 75th percentiles, and whiskers show the 5th and 95th percentiles. The black dots indicate the mean flux rate. Outliers are not displayed.

Figure 5. Averaged seasonality of CO$_2$ and CH$_4$ fluxes in both ecosystems. Dots show daily means across the whole measurement period; lines are a smoothing filter of the daily mean with a 30-day window. Dashed lines show the standard deviation around the daily means, smoothed with a 30-day window.

lake exchange, while there was a strong anti-correlation with sensible heat flux at the lake surface (Table 2), and with solar radiation input (Table 2).

During the thaw seasons, half-hourly CO$_2$ fluxes strongly correlated with CH$_4$ emissions ($\rho = 0.67$, $p < 0.001$, Table 2) and followed the same emission pattern at the half-hourly scale, in both 2013 and 2014 (Fig. S4 in the Supplement). This correlation was not sustained during the open-water seasons, when the two flux datasets had a very different short-
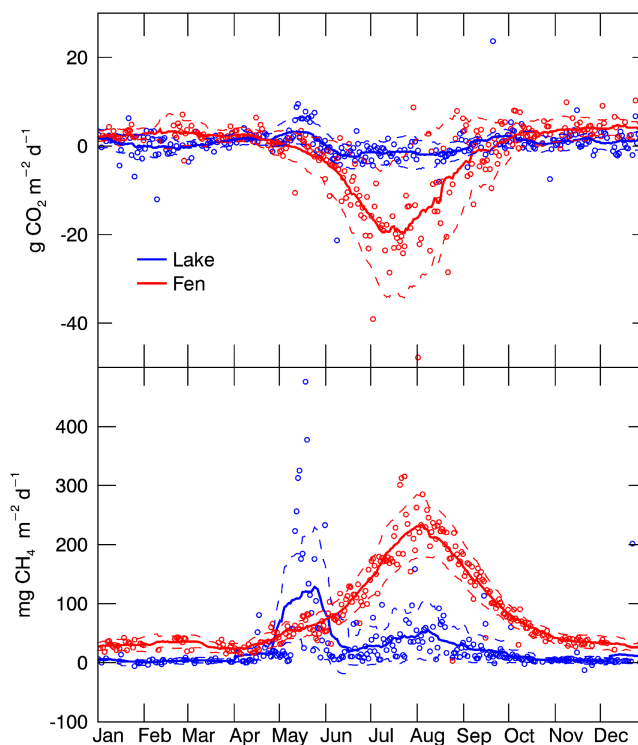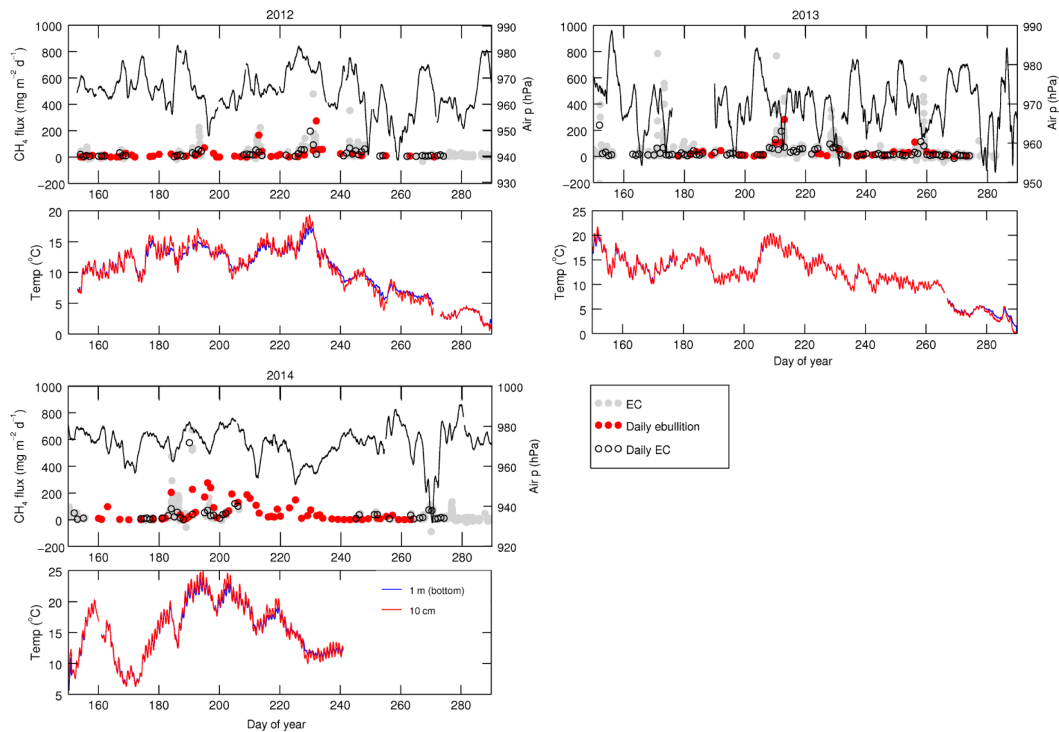
Figure 6. CH$_4$ emissions at the lake during the ice-free seasons of 2012, 2013, and 2014, from day 152 to day 290. Grey dots are half-hourly eddy covariance observations, open black dots are daily means of the eddy covariance fluxes, and red dots show spatially averaged daily CH$_4$ ebullition measured in the lake with bubble traps. Atmospheric pressure (black line), and water temperature at depths 10 cm (red line) and 100 cm (sediment surface, blue line) are also shown.
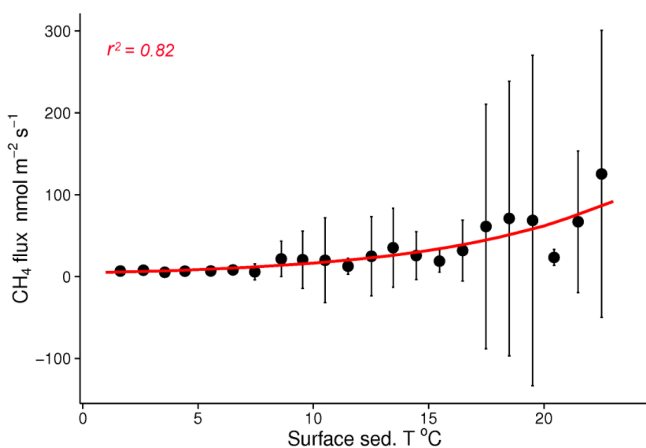

Figure 7. Relationship between lake CH$_4$ emissions and surface sediment temperature during summer, using all half-hourly CH$_4$ flux rates averaged by bins of 1 °C across the three ice-free seasons. Error bars show the standard deviation of the CH$_4$ flux rates around the means within each averaging bin. The red line is a regression fit with $r^2 = 0.82$ ($p < 0.001$).

term variability. Both CH$_4$ and CO$_2$ degassing in spring positively correlated with increasing air temperature.

The diurnal course of CO$_2$, CH$_4$, and turbulent energy fluxes at the lake and the fen was calculated on hourly fluxes. Only days with more than 75 % of hourly data coverage were selected. The median flux of each hour was then computed across all days within each year during the open-water season, and plotted along with the 25th and 75th percentiles (Fig. 8). There was no diel cycle visible in the fen CH$_4$ fluxes, while net CO$_2$ exchange at the fen surface showed a clear peak uptake at noon. Lake methane fluxes tended to be higher fluxes in the morning hours. A systematic diel pattern was observed in the lake CO$_2$ fluxes during each open-water season (Fig. 8), with a slight peak in the mornings in 2012 and 2013, while CO$_2$ uptake peaked in the middle of the day in 2014. The 24 h cycle of sensible heat flux (H) at the lake peaked in the late morning (Fig. 8) at ca. 10:00 LT (median 20 W m^{-2}), while being < 10 W m^{-2} in the afternoon. The diel CO$_2$ pattern at the lake also coincided with daily variation in water surface and air temperature and was in antiphase with the diel pattern of sensible heat flux. Latent heat flux (LE) at the lake peaked in the afternoon. At the hourly timescale, solar radiation could explain 88 % of the diel variability in air–lake CO$_2$ exchange during the summer months
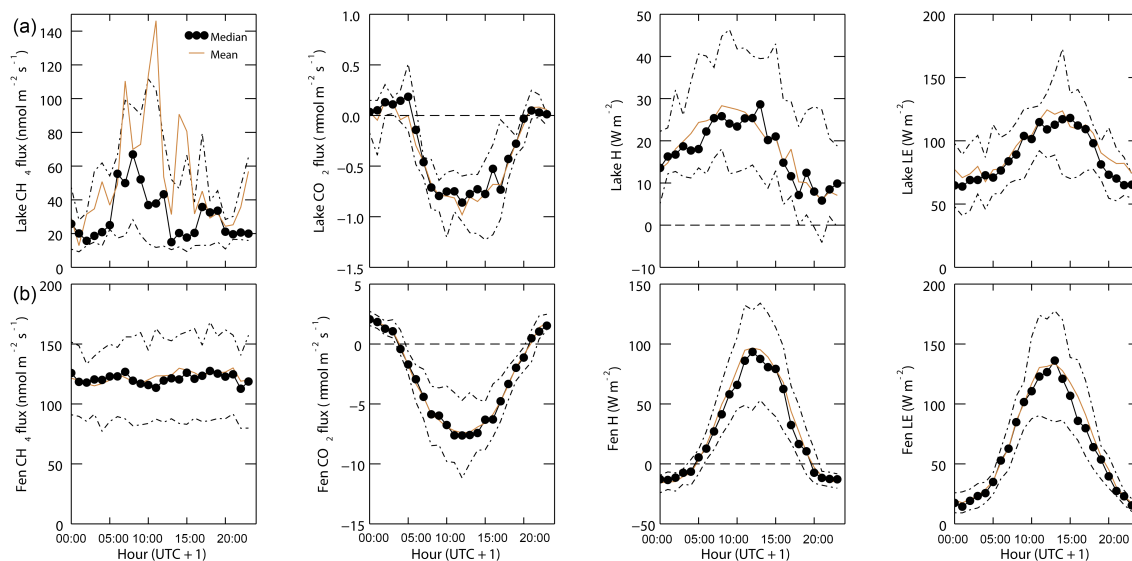
Figure 8. Diel medians, mean and 25th–75th percentiles of CH$_4$ fluxes, CO$_2$ fluxes, sensible heat flux (H) and latent heat flux (LE) measured at the lake **(a)** and at the fen **(b)** from June to August over the three ice-free seasons.
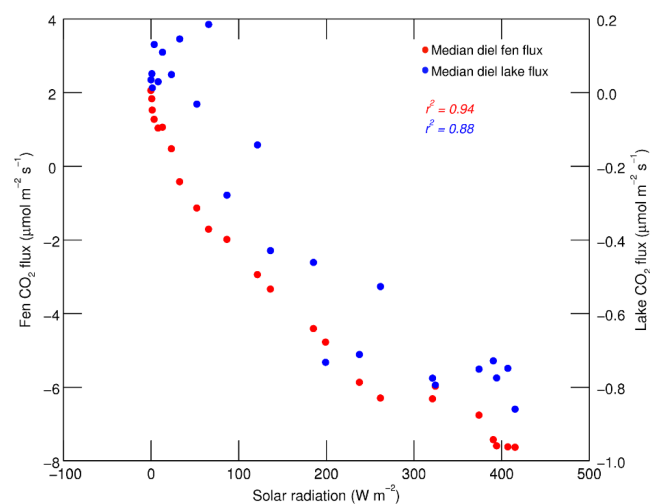

Figure 9. Diel median of the net CO$_2$ exchange at the fen (red) and at the lake (blue) vs. diel median solar radiation, between June and August. Each dot is the hourly median flux of the combined three ice-free seasons. Note that the two y axes have different scales.

(Fig. 9). This light response curve resembled the one measured at the fen, although less pronounced.

3.4 Annual atmospheric carbon budget

3.4.1 Performance of the ANN modeling

The ANN gap filling method was most performant on the fen dataset, achieving an r^2 of 0.88 during the training phase, and an r^2 of 0.85 between measured and predicted values over the whole dataset (expressing the capacity of generaliza-

tion of the model) with a relative mean square error (RMSE) of 23 % (Fig. 10). The ANN gap filling of lake CH$_4$ fluxes achieved an r^2 of 0.71 in the training phase and an r^2 of 0.70 between predicted and measured fluxes on the whole dataset, with an RMSE of 51 %. The lake model was most accurate for periods with the best data coverage in the measured dataset (spring seasons, $r^2 = 0.77$). The lower accuracy of the model during the ice-free seasons ($r^2 = 0.47$) is also due to the pulse character of lake ebullition, which was not always reproduced by the model, while the background seasonal trend was present.

For the fen CH$_4$ fluxes, the model was most accurate during the ice-free seasons when fen CH$_4$ emissions are tightly linked to peat temperature and least performant during the thaw periods. Unsurprisingly, the prediction performance of the models was dependent on data coverage in the original dataset, but also on the accuracy of the choice of environmental drivers. On the annual scale, both fen and lake models were most performant during the first year (June–May), which had the least amount of data loss, with an r^2 of 0.88 (RMSE 23 %) in the first year for the fen model and of 0.82 (RMSE 40 %) for the lake model between predicted and measured fluxes.

The ANN modeling was likewise performant on the fen CO$_2$ flux dataset, achieving an r^2 of 0.86 (RMSE 35 %) over the whole dataset between measured and predicted values (Fig. 10). The model was most performant during the ice-free seasons. This can be explained by a better data coverage but also by better constrained processes during the growing season and on the annual scale than during the snow-cover season, when additional drivers than the one selected as model inputs may play a role in the variability of the fluxes
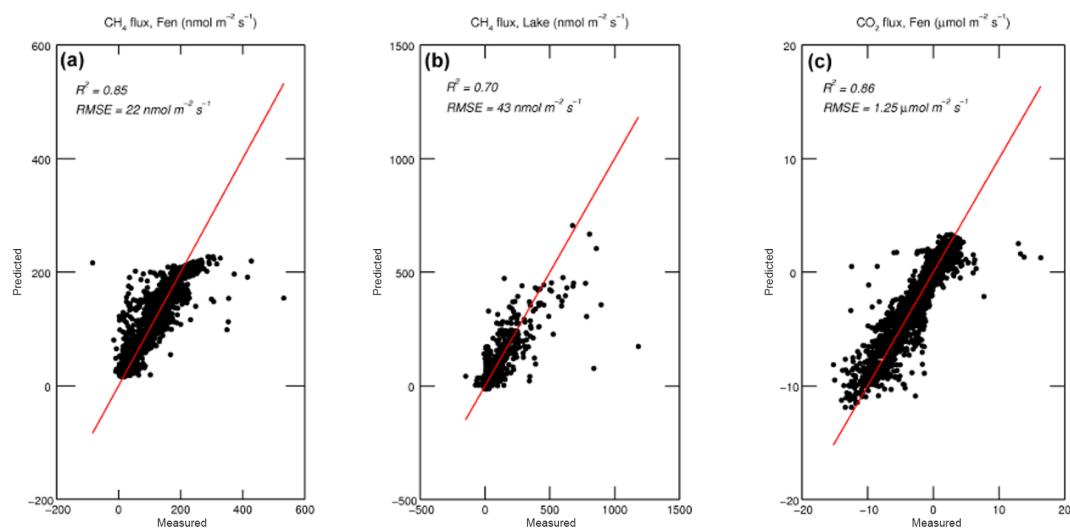
Figure 10. Evaluation of the artificial neural network models: measured vs. predicted hourly flux values for fen CH$_4$ fluxes **(a)**, lake CH$_4$ fluxes **(b)**, and fen CO$_2$ fluxes **(c)**. In red is the 1 : 1 line.

at the hourly scale (e.g., sensitivity to footprint changes, turbulence, variation in snow depth, partial melt).

3.4.2 Annual and seasonal sums

We report seasonal emissions for all available seasons, and for lake CO$_2$ total annual emissions for the first year only (June 2012 to May 2013), due to the absence of a robust gap filling model for the second year when data coverage was lower. During the ice-free seasons, total lake CO$_2$ flux was negative and total lake CH$_4$ flux was positive (Table 3). Annually, the largest contribution to total carbon exchange at the lake was during the spring season, whereas the ice-free season was quantitatively the most important period for the annual carbon exchange at the fen (Table 3). On average over both years, the ice-cover season accounted for 33 % of the fen annual carbon (CH$_4$ + CO$_2$) exchange per m^2. During the first year, the lake C-emissions equaled 70 % of the total net fen C-exchange. On a carbon mass basis, CO$_2$ exchange dominated the total carbon budget. Total net annual carbon exchange (CH$_4$+CO$_2$) at the fen was -38.2 g C m^{-2} in the first year and -52 g C m^{-2} in the second year (average -45.1 g C m^{-2} yr^{-1}), while the lake total carbon exchange was positive at 26.7 g C m^{-2} yr^{-1} (first year only), of which 80 % was emitted as CO$_2$.

4 Discussion

4.1 Contrasting annual seasonality of carbon fluxes between lakes and fens

The average annual seasonality of the fluxes across the study period (Fig. 5) shows that both ecosystems had different peak timings in terms of CH$_4$ and CO$_2$ exchange. CH$_4$ emissions

from the fen followed the expected seasonality of emissions from boreal and subarctic wetlands (Hargreaves et al., 2001; Jackowicz-Korczyński et al., 2010; Rinne et al., 2007). The dense emergent vegetation cover at the waterlogged fen dominated by vascular plants, which are efficient conduits for CH$_4$ to reach the atmosphere, led to maximum primary production of organic carbon during the summer. The continuous emission of CH$_4$ and CO$_2$ through snow during the winter season is an important feature of the annual flux cycle. Unlike the ice cover at the lake, which is complete, stems and branches sticking out of the snow at the fen site allow a sustained connection with the atmosphere. This limits the trapping and the buildup of CH$_4$ under snow during winter. A previous study showed that CH$_4$ emissions from this fen during snowmelt are correlated with air temperature and thus with daily snowmelt and release of trapped gases (Jammet et al., 2015), as seen elsewhere (Friborg et al., 1997; Gažovič et al., 2010). The flux rates during the thaw season were however much lower than during the summer. On the other hand, both CH$_4$ and CO$_2$ fluxes from the lake peaked during the spring season. These pulses coincided with the time of complete water overturn following ice-out on the lake (Fig. 2) and can be explained by the release of gases previously stored in and under lake ice. The annual seasonality was measured from 2.5 years of measurements, and further years of observations are needed to evaluate and explain inter-annual variability in the magnitude of the emissions.

The mean annual CH$_4$ efflux from the lake is in line with a regional estimate of ebullition flux in post-glacial and glacial lakes (32.2 mg CH$_4$ m^{-2} d^{-1}; Wik et al., 2016). Mean fen CH$_4$ fluxes agreed well with chamber measurements conducted over the same period in *Eriophorum*-dominated plots in the Stordalen Mire (P. Crill, unpublished data). The mean CH$_4$ flux measured during the ice-free seasons

is in the upper range of summer CH$_4$ fluxes measured in northern wetlands that are dominated by sedges (ca. 40 to 280 mg CH$_4$ m^{-2} d^{-1}, 25th–95th percentiles, Olefeldt et al., 2013). Measured CO$_2$ flux rates at the fen site also agreed with previous EC studies within the wettest part of the mire (e.g., Christensen et al., 2012) and with flux rates measured with gas chambers in sedge-dominated vegetation plots in previous years (Bäckstrand et al., 2010) and during the study period (P. Crill, unpublished data), at the seasonal and annual scales. The fen is thus representative of minerotrophic northern fens where high CH$_4$ emissions are measured due to year-round anoxia in the soil and due to the dominance of vascular plants (Olefeldt et al., 2013). Lakes that freeze solid in winter are not expected to emit a significant amount of CO$_2$ at the surface, unless ice-free holes caused by strong bubble seeps are present (e.g., Sepulveda-Jauregui et al., 2015), which we do not observe in the lakes of Stordalen (Wik et al., 2011). The observation of CO$_2$ fluxes from the lake during the second winter at rates that are within the magnitude of land winter respiration (Fig. 3) was thus unexpected. The high winter flux rates were coincident with strong winds, increasing air temperature, and high latent heat flux. Whether these are due to a physical evasion of CO$_2$ through snow over the lake surface or due to lateral advection of land-emitted CO$_2$ is unclear. Increased ambient CO$_2$ concentration over the lake in winter may be an indication of non-turbulent transport of CO$_2$ from land. Indeed, the extended flux footprint in winter might include part of the land in the middle of the lake, leading to vegetation-like flux magnitudes. Although this effect was limited by filtering for large wind dispersion during winter periods, part of the flux could still be influenced by land respiration to an extent that we cannot quantify.

During the summer, the low magnitude of CO$_2$ fluxes from the lake resulted in a low signal-to-noise ratio (high relative random error). The uncertainty linked to the inclusion of low-frequency contributions is a problem that has been discussed widely in the eddy covariance community, particularly for low-flux environments (e.g., Sievers et al., 2015). Testing CO$_2$ flux calculation with a new method that removes the low-frequency contributions (Sievers et al., 2015) on a portion of our data in July 2012 showed nevertheless that the summer fluxes at the lake were coincident with our measurement, with a negative mean and diel pattern with slight uptake during the day (J. Sievers, personal communication, 2016). This indicates that despite a high noise our CO$_2$ lake flux measurements during summer are trustworthy. In addition, the flux footprint was representative of each ecosystem (lake vs. fen). The diel patterns of sensible and latent heat fluxes from the lake resembled those observed in boreal lakes (Mammarella et al., 2015; Nordbo et al., 2011; Shao et al., 2015; Vesala et al., 2006), which further supports our EC measurement from the eastern sector being representative of the lake surface. Overall, CO$_2$ fluxes in the context of a low-flux environment such as this lake should be interpreted with care; we provide here the best estimate possible with the available instrumentation at the time of the study.

4.2 Season-dependent transport pathways of CH$_4$ and CO$_2$ from the lake to the atmosphere

4.2.1 Ice-free season

Eddy covariance measures a direct flux across the surface–atmosphere interface, spatially integrating over m^2 to km^2 all emitting pathways that are responsible for the transport of gas from the ecosystem to the atmosphere (i.e., total flux). In this study, CH$_4$ emissions from the lake during the ice-free seasons were dominated by short, large degassing events (Figs. 3, C1) that coincided with drops in atmospheric pressure. Furthermore, daily EC observations coincided with spatially averaged ebullition fluxes measured with bubble traps (Fig. 6), which supports CH$_4$ fluxes being representative of the lake surface. These observations also suggest that the total CH$_4$ efflux from the lake during the ice-free seasons was mostly due to the release of bubbles formed in the sediments (ebullition), in line with previous observations that ebullition is the main pathway for CH$_4$ emissions in shallow lake areas (Bastviken et al., 2004).

A strong relationship was found between CH$_4$ efflux and surface sediment temperature; thus, the slight seasonality in summer CH$_4$ emissions from the lake (Fig. 5) is likely due to the seasonal increase in temperature in the production zone. This seasonal trend also supports a bubble release mechanism, since a seasonal increase in sediment temperature favors methanogenesis and additionally causes a decrease in CH$_4$ solubility (Casper et al., 2000; Wik et al., 2013). This suggests that the amount of CH$_4$ emitted at the lake surface is directly linked to the amount of CH$_4$ produced within the sediments, as has been observed using bubble traps (Wik et al., 2014). A significant relationship between bubble flux and surface sediment temperature similar to the one we reported here was observed in the lakes of the Stordalen catchment by Wik et al. (2014), who identified the threshold for ebullition in the Stordalen lakes at 6 °C. Our EC system measures fluxes for sediment temperatures under 6 °C, which could be diffusive. The occasional occurrence of degassing during summer that timed up with short de-stratification events (Fig. S3 in the Supplement) indicates that hydrodynamic transport and diffusion of CH$_4$ linked to lake mixing may happen in this lake, as has been observed in a boreal lake (Podgrajsek et al., 2014). Water currents can also trigger bubble release by disturbing surface sediments (Joyce and Jewell, 2003).

Exchange of CO$_2$ across the lake–air interface is mainly diffusion-limited due to the temperature of dissolution of CO$_2$ in water, which does not favor the release of CO$_2$ in bubbles (Tranvik et al., 2009). On average, the net CO$_2$ flux at the surface of the lake during the ice-free seasons revealed photosynthetic activity. The strong light response curve of

median diel emissions (Fig. 9) is largely influenced by flux rates measured during the warm, sunny summer of 2014. The presence of the diel pattern in summertime CO_2 fluxes was tested for the influence of advection from the lake shore by recalculating the fluxes from the lake using a 5 min average instead of 30 min (Eugster, 2003; Podgrajsek et al., 2015; Vesala et al., 2006). The pattern persisted for 5 min averaged fluxes during the summer of 2012 (Fig. S5 in the Supplement), which suggests that advection had a small effect on the summer CO_2 fluxes.

CO_2 uptake at the lake in summer was associated with unstable atmospheric conditions and positive H (Table 2). Waterside convection due to cooling of the lake surface has been shown to enhance the diffusion-limited exchange of CO_2 (Eugster, 2003; Podgrajsek et al., 2015). If the lake water is under-saturated in CO_2 with respect to the atmosphere, this results in a downward CO_2 flux. The anti-correlation we observe between CO_2 flux and H during summer could thus be due to the diffusive CO_2 flux between the surface and the atmosphere being enhanced by convection near the lake surface. Diel patterns in CO_2 flux linked to lake mixing have been observed in other eddy covariance studies, where they are associated with a release of CO_2 into the atmosphere (Mammarella et al., 2015; Podgrajsek et al., 2015).

Finally, the low burst of CO_2 observed in fall 2014 may be the result of an accumulation of CO_2 during the warmer summer 2014, when sustained warm temperatures could cause a thermal stratification of the lake at the end of the season. When lake cooling in fall triggers water mixing, accumulated gases at the lake bottom can be released to the atmosphere (e.g., Kankaala et al., 2006). In other years, regular mixing of the lake during summer may have prevented this phenomenon from occurring.

4.2.2 Thaw season

The strong correlation of CH_4 and CO_2 emissions at the lake during both spring periods suggests that the gases were emitted into the atmosphere via the same mechanism, i.e., by turbulence-driven release of gases that have been accumulating in the lake. Conversely, the correlation is very low during the ice-free periods, when ebullition is the dominant process of CH_4 release. The outgassing pattern at thaw coincided in both years with the breakdown of thermal stratification in the water column after complete ice disappearance. Bubbles trapped in the winter ice of lake Villasjön contain both CH_4 and CO_2 (Boereboom et al., 2012). CO_2 stored in lake ice during winter can originate from benthic respiration which can occur under ice while dead plants from the previous summer are decomposing (Karlsson et al., 2008). Methanotrophy can be important during overturn events in lakes (Kankaala et al., 2006; Schubert et al., 2012); thus, CO_2 may also be produced in lake water during ice thaw, which lasts several days, as an output of CH_4 oxidation. Dissolved CO_2 could

also enter the lake as catchment input via lateral meltwater run-off before complete overturn (Denfeld et al., 2015).

The processes underlying CH_4 degassing during thaw in 2013 have been discussed in detail in a previous study (Jammet et al., 2015), suggesting that the spring burst is the combination of different gas sources, i.e., liberation of bubbles from the ice, diffusion of gases from the water to the air, and release of stored gases from the bottom of the lake during complete overturn. As CO_2 fluxes covariate closely with CH_4 emissions from the lake during spring (Fig. S4 in the Supplement), it is likely that CO_2 was released via the same physical mechanisms. The degassing pattern observed in 2013 was repeated in 2014, with a mean and median CH_4 flux rate smaller than the previous year but still significantly higher than the CH_4 emissions of the ice-free season (Fig. S2 in the Supplement). In 2014 the thaw period started earlier but was longer (Fig. 2), and our measurement system may have missed part of the degassing due to instrument failure. As ice thaws, gases contained in bubbles can migrate to the water (Greene et al., 2014) and be released into the atmosphere when thermal stratification gradually breaks because of the warming up of the water column. We can speculate that a delay in the timing of overturn following ice thaw may favor oxidation of CH_4 within the water column when it is already partly mixing, which would raise the concentration of dissolved CO_2 in the water and could contribute to a smaller burst of CH_4 during complete overturn.

4.3 Annual atmospheric carbon budget

4.3.1 Carbon function

The fen was an annual sink of carbon with respect to the atmosphere, while the lake was an annual source, at a magnitude representing 70 % of the fen sink. The total annual C-emission from the lake is within the range of annual C-emissions ($CH_4 + CO_2$) from lakes of subarctic Sweden (5 to 54 g C m^{-2} yr^{-1}, Lundin et al., 2015) estimated mostly using water grab sampling.

At the fen, we report a stronger summer sink of CO_2 (three ice-free seasons average -206.8 g C m^{-2}, Table 3) compared to earlier studies in the inner fens of the Stordalen mire (-133 g C m^{-2}, years 2001–2008, Christensen et al., 2012), but annually a net CO_2 uptake (-58.5 to -79.1, average -66.3 g C m^{-2} yr^{-1}) that is similar to the 2001–2008 average (-66 g C–CO_2 m^{-2} yr^{-1}, Christensen et al., 2012) and smaller than the average for years 2006–2008, which were warm years (-90 g C–CO_2 m^{-2} yr^{-1}, Christensen et al., 2012). The difference is due to the higher CO_2 respiration we measured in winter, which equaled 54 % of the summer sink on average during the measuring period. The annual CH_4 emissions of 21.2 C–CH_4 m^{-2} yr^{-1} (Table 3) are very close to what has been reported for the internal fens of Stordalen in an eddy covariance study where winter emissions were estimated with a temperature relation-

ship (Jackowicz-Korczyński et al., 2010). This highlights the stability of the fen in terms of CH$_4$ emissions, but also the low sensitivity of the annual sum to the choice of gap filling method for the fen CH$_4$ flux dataset, which is tightly linked to temperature.

To determine whether an ecosystem is a net source or sink of carbon within the landscape carbon cycling, a full net ecosystem carbon balance (NECB) must take into account not only vertical carbon exchange, but also lateral carbon transport, in and out of the system (Chapin et al., 2006). In 2008, net DOC export at the fen was 8.1 g C m^{-2} yr^{-1} and net POC export was 0.6 g C m^{-2} yr^{-1} (Olefeldt and Roulet, 2012). Combined with our annual atmospheric carbon budget (Table 3), this results in a fen NECB of -29.5 g C m^{-2} yr^{-1} in the first year and -43.3 g C m^{-2} yr^{-1} in the second year. These numbers are marginally smaller than the long-term carbon accumulation of -51 g C m^{-2} yr^{-1} inferred from the analysis of a peat cored in Stordalen and attributed to a period when the mire was dominated by graminoids (Kokfelt et al., 2010). We are not aware of existing data on net export of DOC and POC through the lake to make a similar estimate.

In terms of radiative forcing, considering the 28-fold stronger global warming potential of atmospheric CH$_4$ vs. atmospheric CO$_2$ over 100 years (GWP100, Myhre et al., 2013), vertical carbon exchange has a warming impact on the atmosphere at both ecosystems through their net annual emissions of CH$_4$. Annual estimates that disregard winter and transitional seasons are likely missing part of the annual carbon emissions from seasonally freezing lakes and wetlands.

4.3.2 The lake as a summer CO$_2$ sink

Because of dynamic external and internal factors governing the consumption and production of CO$_2$ in surface waters, the CO$_2$ function of a lake can vary seasonally (Maberly, 1996; Shao et al., 2015). Lake Villasjön was an annual source of CO$_2$ due to the spring outgassing, but it was a small sink of CO$_2$ in the open-water period. While flux rates in summers 2012 and 2013 were negative but close to the noise level, the uptake was larger and significant in 2014 when the summer was hotter and sunnier. Averaged estimates from water sampling measurements in the lakes of the Abisko area indicate the lakes to be mainly CO$_2$ sources during the summer, except for a few lakes that were seasonal CO$_2$ sinks during the ice-free season (Karlsson et al., 2013). In the few eddy covariance studies available from Arctic and boreal sites, lakes are reported as CO$_2$ sources during the ice-free season (Lohila et al., 2015; Mammarella et al., 2015; Podgrajsek et al., 2015) and occasional CO$_2$ sinks during the warm summer months, while being sources on the seasonal scale (Anderson et al., 1999; Eugster, 2003; Huotari et al., 2011; Jonsson et al., 2008). No coincident measurement of pCO$_2$ in the lake water is available for the study period. A future study com-

bining pCO$_2$ with EC will help further define the direction of the flux observed on the ecosystem scale.

Although Villasjön is representative of a widespread post-glacial lake type across subarctic and Arctic latitudes, it differs from most lakes studied in the northern lakes literature due to its particularly shallow depth, which results in the lack of long-term stratification during the open-water season. Lakes that are similarly shallow are often thermokarst lakes or peatland ponds (Vonk et al., 2015). Summer CO$_2$ uptake at the level of what we report here has been observed in highly productive lakes (Pacheco et al., 2013) or in thaw ponds colonized by submerged plants and microbial mats (Laurion et al., 2010; Tank et al., 2009). Estimates of air–lake carbon exchange using water sampling and floating chambers (Karlsson et al., 2013) showed that a minority of lakes in subarctic Sweden were CO$_2$ sinks in summer, with a total seasonal CO$_2$ exchange from -3.8 to -10 g C m^{-2} yr^{-1}, while being large sources at ice-out, offsetting the summer sink.

Lakes with poor hydrological connections with their upstream catchment have been reported in previous studies to be net CO$_2$ sinks in summer, e.g., in Minnesota (Striegl and Michmerhuizen, 1998) or in thaw ponds of the Canadian Arctic (Tank et al., 2009). In the latter study, within-lake DOC was proposed to occur as a byproduct of macrophyte photosynthesis, showing that net CO$_2$ uptake in lakes is not always associated with low DOC concentrations. In large and shallow lakes surrounded by peatlands, vegetation develops on the sediment surface thanks to the presence of humic acids supplied by the peaty shores and a well-illuminated bottom (Banaś et al., 2012). The analysis of peat and lake sediment records in Stordalen suggested that a significant amount of peat is exported from the mire to lake Villasjön during periods of mire erosion, likely due to permafrost thaw (Kokfelt et al., 2010). This lake may have high nutrient content due to peat input at the shores, organic-rich sediments, and autochthonous vegetation. Lakes that do not stratify tend to be more productive because of the more regular mixing of nutrients (Tranvik et al., 2009; Wetzel, 2001).

4.3.3 Influence of overturn on annual C-emissions

On an annual scale, the thaw period accounted for 50 % of annual carbon exchange (CH$_4$ + CO$_2$) at lake Villasjön and turned the lake from a summer CO$_2$ sink into an annual source. In other, deeper lakes that stratify in summer and do not fully mix in spring, fall overturn led to the highest emissions of CH$_4$ or CO$_2$ of the year (Kankaala et al., 2006; Schubert et al., 2012), accounting for a large part of the annual CO$_2$ flux (Huotari et al., 2011). Other seasonally ice-covered lakes emitted large amounts of CH$_4$ and CO$_2$ following ice-out (Anderson et al., 1999; Karlsson et al., 2013), while high concentrations of dissolved CO$_2$ and CH$_4$ under lake ice have been measured in North American lakes (Striegl and Michmerhuizen, 1998), across lakes of the Swedish subarctic (Karlsson et al., 2013), in Alaskan thermokarst lakes

(Sepulveda-Jauregui et al., 2015), or in thaw ponds in Canada (Tank et al., 2009). Accumulation of CH_4 and CO_2 under the ice is thus a general feature of lakes with an anoxic hypolimnion or sediment in winter, but studies reporting direct measurement of the outgassing of CH_4 and CO_2 at the lake surface right after thaw are scarce because it is a rapid and variable phenomenon that is seldom included in direct flux measurements.

The large impact of CO_2 and CH_4 release during spring has been observed in lakes of the Abisko area where water samples before and after ice-out were used to estimate the thaw release, which accounted on average for 45 % of annual emissions (Karlsson et al., 2013; Lundin et al., 2013). A few regional studies reported on a lesser importance of the spring season for annual carbon emissions from lakes. Sepulveda-Jauregui et al. (2015) sampled 40 Alaskan thermokarst lakes where the maximum emissions of CH_4 and CO_2 were measured in summer. Many of these lakes were thermokarst lakes that continuously emitted CH_4 in winter through open holes, which we do not observe in lake Villasjön. Thermokarst lakes are usually stronger CH_4 emitters than post-glacial lakes on a per unit area basis, yet post-glacial lakes seem to be a larger overall source because they cover a larger area at the high northern latitudes (Wik et al., 2016). A recent review by Wik et al. (2016) compiled CH_4 emissions from several types of lakes. Over the total of 733 sites, the thaw period was estimated to contribute ~ 23 % of annual emissions of lakes and ponds. Only four sites were measured with EC, and those four only comprised ice-free season (July–August) measurements. Thus the comparison to our results is limited by differences in the temporal and spatial scale of the methods.

Our study underlines the high significance of shoulder seasons (more precisely, overturn periods following periods of gas storage) for the biogeochemistry of lakes and the emission of CO_2 and CH_4 into the atmosphere. The relative importance of these periods for the annual emissions depends on the extent of the overturn (Huotari et al., 2011; Kankaala et al., 2006), the extent of methanotrophy during and before full lake mixing (Kankaala et al., 2006; Schubert et al., 2012), as well as the amount of degradable organic matter in the hypolimnion. Although these overturn periods cover only a few weeks or days, they are important for both CH_4 and CO_2 emissions in lakes and should be included in measurement campaigns when feasible.

5   Conclusions

The waterlogged fen and the shallow lake showed contrasting annual cycles in terms of CH_4 and CO_2 exchange with the atmosphere. This difference is explained, first, by the presence of an ice lid over the lake surface which led to the storage of gases in winter and large subsequent emissions in spring, while evasion of CH_4 and CO_2 to the atmosphere from the fen in the wintertime limits the importance of emissions dur-

ing ice melt and snowmelt. Second, the dense cover of vascular plants at the fen leads to high CH_4 emissions and CO_2 uptake in summer.

Annually, the fen was a net carbon sink with respect to the atmosphere, while the lake was a source of carbon due to the degassing in spring that outweighed the apparent uptake of CO_2 in summer. This study confirms the importance of overturn periods in lakes for both CH_4 and CO_2 annual emissions. The magnitude of the degassing during the thaw season may depend greatly on lake type, morphometry, and productivity status. The lake studied represents a common type of shallow post-glacial lake across the subarctic latitudes. Further direct measurements of surface fluxes covering several years and different lake types are needed to evaluate the inter-annual variability in the magnitude of the degassing in shoulder seasons as well as its importance for the annual emissions of northern lakes in general.

Finally, ebullition was identified as the main transport pathway for CH_4 emissions in the shallow subarctic lake, and a net CO_2 sink in summer indicated photosynthetic activity. Turbulence-driven diffusive release of CO_2 and CH_4 was predominant during spring overturn following ice-out. These results show the potential of the EC method in lake environments for a better understanding of flux processes and annual seasonality in the understudied but abundant post-glacial lakes and ponds.

Appendix A: Details in eddy covariance flux calculation

Processing of the raw eddy covariance data for flux calculation included despiking (Vickers and Mahrt, 1997), angle of attack correction on raw wind components (Nakai et al., 2006), 2-D axis rotation (Wilczak et al., 2001) on wind speed components, and detrending of 30 min raw data intervals by block averaging the vertical wind speed and scalar signals (Moncrieff et al., 2004). The time delay between vertical wind speed and gas concentration measurements (CO$_2$, CH$_4$, H$_2$O) was removed by finding the maximum of the cross-covariance function of vertical wind speed and each scalar (Fan et al., 1990). The time-window search was set to $\pm 4\,s$ for CO$_2$ and H$_2$O; the median time lag was 0 s. For CH$_4$, the time-window search was adjusted for each period when a change in the setup occurred; the median time lag between vertical wind speed and CH$_4$ concentration measurements varied between 9 and 18 s.

The effect of density fluctuations on CO$_2$ fluxes was corrected (Webb et al., 1980). The correction lowered the amplitude of the CO$_2$ flux dataset on average by 53% (slope of the linear regression between non-density corrected CO$_2$ fluxes and final corrected fluxes $= 0.47$, $r^2 = 0.73$). Due to the unavailability of H$_2$O concentration measurements from the methane analyzer during most of the study period, WPL correction was not applied by the flux software on CH$_4$ fluxes. Applying the correction on part of the data using the available H$_2$O concentration from the methane analyzer showed a difference in flux magnitude of about 1 % with the non-corrected dataset. The low magnitude of the WPL correction can be expected for this setup, due to the long sampling line that attenuates significantly the H$_2$O signal as well as temperature and pressure fluctuations, and thus density effects. Turbulent fluxes calculated with the eddy covariance method are affected by spectral losses due to the instrumental setup and the limited time response of the instruments. Losses in the low-frequency range due to the finite flux averaging time were corrected analytically after Moncrieff et al. (2004). CO$_2$ flux loss in the high-frequency range was also corrected analytically (Moncrieff et al., 1997), while CH$_4$ fluxes derived from the closed-path system required an in situ assessment of the system's cut-off frequency (Ibrom et al., 2007) due to the long sampling line. This assessment was done separately for each period with a continuous instrumental setup and the associated flux attenuation was calculated and compensated following the formulation by Horst (1997). The magnitude of the spectral loss and hence of the total spectral correction was on average 31 % for CO$_2$ fluxes and 37 % for CH$_4$ fluxes.

Appendix B: Computing the performance of the ANN models

The performance of the ANN models was assessed by comparing the predicted values with original observed values of the entire dataset (Table B1). This represents the actual ability of the ANN to generalize (Papale and Valentini 2003) to untrained conditions. The goodness of fit was quantified with the coefficient of determination r^2 and the root mean square error (RMSE). Additionally, the mean random error of the predicted flux values was calculated as the mean of the standard deviation around each individual value used for gap filling. In other words: each modeled value used for gap filling is the mean of several ANN model runs. The 25 best runs (according to r^2) were averaged to obtain the modeled fluxes used in the gap filling. The standard deviation of these 25 model outputs was thus used as a quantification of the random error of each modeled flux value. The average of these individual random errors was then computed as the mean random error of each modeled flux series (CH$_4$ fen, CH$_4$ lake, CO$_2$ fen) reported in Table B1.

Table B1. Characteristics of the artificial neural networks that were developed for gap filling fen and lake CH$_4$ fluxes and fen CO$_2$ fluxes. All networks were developed with one hidden layer and with four fuzzy datasets as additional input to force seasonality. The mean random error is the average of the standard deviation around the modeled flux values for each series (cf. Text S1 in the Supplement).

	Fen CH$_4$	Fen CO$_2$	Lake CH$_4$
Input variables	T_{air}	Photosynthetic active radiation (PAR)	T_{air}
	T_{peat} at 10 cm	T_{air}	T water at 10 cm
	Wind speed	Vapour pressure deficit	T in sediment surface (100 cm)
	Air pressure	(VPD)	Wind speed
	Net radiation (fen)	Net radiation (fen)	Air pressure
	Incoming solar radiation		Net radiation (lake)
			Incoming solar radiation
Number of neurons	6	6	9
R2 (all predicted vs. obs.)	0.85	0.86	0.70
RMSE (all predicted vs. obs., μmol m^{-2} s^{-1})	0.022	1.25	0.043
Mean random error of all predicted values (μmol m^{-2} s^{-1})	0.004	1.3	0.011

Appendix C
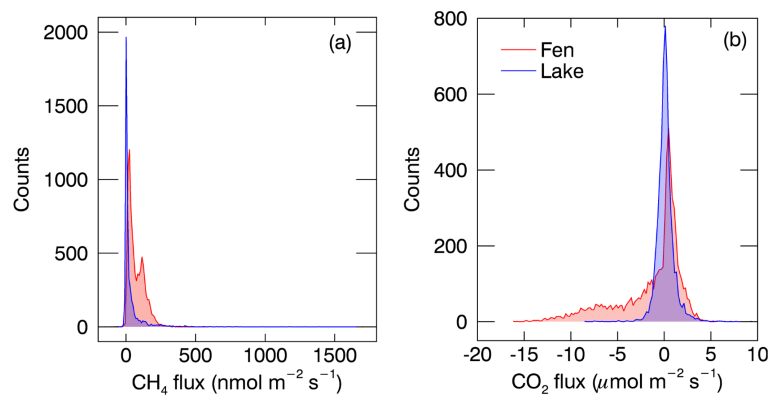
Figure C1. Probability density functions of **(a)** the measured CH$_4$ fluxes (bin size 10 nmol m^{-2} s^{-1}) and **(b)** the measured CO$_2$ fluxes (bin size 0.2 µmol m^{-2} s^{-1}) from the fen and from the lake during the entire measurement period.

Author contributions. TF, MJ, and PC designed the study. MJ collected, analyzed, and interpreted the data. SD developed and performed the gap filling modeling. EK pre-processed part of the eddy covariance raw data. FJWP performed the 2-D footprint modeling and drew the footprint figure. MW provided methane ebullition data. MJ wrote the manuscript and figures and all authors commented on them.

Competing interests. The authors declare that they have no conflict of interest.

Special issue statement. This article is part of the special issue "Interactions between climate change and the Cryosphere: SVALI, DEFROST, CRAICC (2012–2016) (TC/ACP/BG inter-journal SI)". It is not associated with a conference.

References

Åkerman, H. J. and Johansson, M.: Thawing permafrost and thicker active layers in sub-arctic Sweden, Permafrost Periglac., 19, 279–292, https://doi.org/10.1002/ppp.626, 2008.

Algesten, G., Sobek, S., Bergström, A.-K., Ågren, A., Tranvik, L. J., and Jansson, M.: Role of lakes for organic carbon cycling in the boreal zone, Glob. Change Biol., 10, 141–147, https://doi.org/10.1111/j.1365-2486.2003.00721.x, 2004.

Anderson, D. E., Striegl, R. G., Stannard, D. I., Michmerhuizen, C. M., McConnaughey, T. A., and LaBaugh, J. W.: Estimating lake-atmosphere CO$_2$ exchange, Limnol. Oceanogr., 44, 988–1001, 1999.

Aubinet, M., Vesala, T., and Papale, D. (Eds.): Eddy Covariance, Springer Netherlands, Dordrecht, available at: http://link.springer.com/10.1007/978-94-007-2351-1 (last access: 24 September 2014), 2012.

Bäckstrand, K., Crill, P. M., Jackowicz-Korczyñski, M., Mastepanov, M., Christensen, T. R., and Bastviken, D.: Annual carbon gas budget for a subarctic peatland, Northern Sweden, Biogeosciences, 7, 95–108, https://doi.org/10.5194/bg-7-95-2010, 2010.

Banaś, K., Gos, K., and Szmeja, J.: Factors controlling vegetation structure in peatland lakes—Two conceptual models of plant zonation, Aquat. Bot., 96, 42–47, https://doi.org/10.1016/j.aquabot.2011.09.010, 2012.

Bastviken, D., Cole, J., Pace, M., and Tranvik, L.: Methane emissions from lakes: Dependence of lake characteristics, two regional assessments, and a global estimate, Global Biogeochem. Cy., 18, GB4009, https://doi.org/10.1029/2004GB002238, 2004.

Bastviken, D., Tranvik, L. J., Downing, J. A., Crill, P. M., and Enrich-Prast, A.: Freshwater methane emissions offset the continental carbon sink, Science, 331, p. 50, https://doi.org/10.1126/science.1196808, 2011.

Battin, T. J., Luyssaert, S., Kaplan, L. A., Aufdenkampe, A. K., Richter, A., and Tranvik, L. J.: The boundless carbon cycle, Nat. Geosci., 2, 598–600, https://doi.org/10.1038/ngeo618, 2009.

Boereboom, T., Depoorter, M., Coppens, S., and Tison, J.-L.: Gas properties of winter lake ice in Northern Sweden: implication for carbon gas release, Biogeosciences, 9, 827–838, https://doi.org/10.5194/bg-9-827-2012, 2012.

Brix, H., Sorrell, B. K., and Orr, P. T.: Internal pressurization and convective gas flow in some emergent freshwater macrophytes, Limnol. Oceanogr., 37, 1420–1433, https://doi.org/10.4319/lo.1992.37.7.1420, 1992.

Bubier, J., Crill, P., and Mosedale, A.: Net ecosystem CO$_2$ exchange measured by autochambers during the snow-covered season at a temperate peatland, Hydrol. Process., 16, 3667–3682, https://doi.org/10.1002/hyp.1233, 2002.

Burba, G. G., McDermitt, D. K., Grelle, A., Anderson, D. J., and Xu, L.: Addressing the influence of instrument surface heat exchange on the measurements of CO$_2$ flux from open-path gas analyzers, Glob. Change Biol., 14, 1854–1876, https://doi.org/10.1111/j.1365-2486.2008.01606.x, 2008.

Callaghan, T. V., Bergholm, F., Christensen, T. R., Jonasson, C., Kokfelt, U., and Johansson, M.: A new climate era in the sub-Arctic: Accelerating climate changes and multiple impacts, Geophys. Res. Lett., 37, L14705, https://doi.org/10.1029/2009GL042064, 2010.

Casper, P.: Methane production in lakes of different trophic state, Arch. Hydrobiol. Beih. Ergebn. Limnol., 37, 149–154, 1992.

Casper, P., Maberly, S. C., Hall, G. H., and Finlay, B. J.: Fluxes of methane and carbon dioxide from a small productive lake to the atmosphere, Biogeochemistry, 49, 1–19, https://doi.org/10.1023/A:1006269900174, 2000.

Chapin, F. S., Woodwell, G. M., Randerson, J. T., Rastetter, E. B., Lovett, G. M., Baldocchi, D. D., Clark, D. A., Harmon, M. E., Schimel, D. S., Valentini, R., Wirth, C., Aber, J. D., Cole, J. J., Goulden, M. L., Harden, J. W., Heimann, M., Howarth, R. W., Matson, P. A., McGuire, A. D., Melillo, J. M., Mooney, H. A., Neff, J. C., Houghton, R. A., Pace, M. L., Ryan, M. G., Running, S. W., Sala, O. E., Schlesinger, W. H., and Schulze, E.-D.: Reconciling Carbon-cycle Concepts, Terminology, and Methods,

Ecosystems, 9, 1041–1050, https://doi.org/10.1007/s10021-005-0105-7, 2006.

Christensen, T. R.: Thawing sub-arctic permafrost: Effects on vegetation and methane emissions, Geophys. Res. Lett., 31, L04501, https://doi.org/10.1029/2003GL018680, 2004.

Christensen, T. R., Ekberg, A., Ström, L., Mastepanov, M., Panikov, N., Öquist, M., Svensson, B. H., Nykänen, H., Martikainen, P. J., and Oskarsson, H.: Factors controlling large scale variations in methane emissions from wetlands, Geophys. Res. Lett., 30, 1414, https://doi.org/10.1029/2002GL016848, 2003.

Christensen, T. R., Jackowicz-Korczyński, M., Aurela, M., Crill, P., Heliasz, M., Mastepanov, M., and Friborg, T.: Monitoring the Multi-Year Carbon Balance of a Subarctic Palsa Mire with Micrometeorological Techniques, AMBIO, 41, 207–217, https://doi.org/10.1007/s13280-012-0302-5, 2012.

Cicerone, R. J. and Oremland, R. S.: Biogeochemical aspects of atmospheric methane, Global Biogeochem. Cy., 2, 299–327, https://doi.org/10.1029/GB002i004p00299, 1988.

Cole, J. J. and Caraco, N. F.: Atmospheric exchange of carbon dioxide in a low-wind oligotrophic lake measured by the addition of SF6, Limnol. Oceanogr., 43, 647–656, doi:10.4319/lo.1998.43.4.0647, 1998.

Cole, J. J., Prairie, Y. T., Caraco, N. F., McDowell, W. H., Tranvik, L. J., Striegl, R. G., Duarte, C. M., Kortelainen, P., Downing, J. A., Middelburg, J. J., and Melack, J.: Plumbing the global carbon cycle: Integrating inland waters into the terrestrial carbon budget, Ecosystems, 10, 172–185, https://doi.org/10.1007/s10021-006-9013-8, 2007.

Cory, R. M., Ward, C. P., Crump, B. C., and Kling, G. W.: Sunlight controls water column processing of carbon in arctic fresh waters, Science, 345, 925–928, https://doi.org/10.1126/science.1253119, 2014.

Crill, P. M., Bartlett, K. B., Harriss, R. C., Gorham, E., Verry, E. S., Sebacher, D. I., Madzar, L., and Sanner, W.: Methane flux from Minnesota Peatlands, Global Biogeochem. Cy., 2, 371–384, https://doi.org/10.1029/GB002i004p00371, 1988.

Dee, D. P., Uppala, S. M., Simmons, A. J., Berrisford, P., Poli, P., Kobayashi, S., Andrae, U., Balmaseda, M. A., Balsamo, G., Bauer, P., Bechtold, P., Beljaars, A. C. M., van de Berg, L., Bidlot, J., Bormann, N., Delsol, C., Dragani, R., Fuentes, M., Geer, A. J., Haimberger, L., Healy, S. B., Hersbach, H., Hólm, E. V., Isaksen, L., Kållberg, P., Köhler, M., Matricardi, M., McNally, A. P., Monge-Sanz, B. M., Morcrette, J.-J., Park, B.-K., Peubey, C., de Rosnay, P., Tavolato, C., Thépaut, J.-N., and Vitart, F.: The ERA-Interim reanalysis: configuration and performance of the data assimilation system, Q. J. Roy. Meteor. Soc., 137, 553–597, https://doi.org/10.1002/qj.828, 2011.

Denfeld, B., Wallin, M. B., Sahlée, E., Sobek, S., Kokic, J., Chmiel, H. E., and Weyhenmeyer, G. A.: Temporal and spatial carbon dioxide concentration patterns in a small boreal lake in relation to ice cover dynamics, ResearchGate, 20, 679–692, 2015.

Dengel, S., Zona, D., Sachs, T., Aurela, M., Jammet, M., Parmentier, F. J. W., Oechel, W., and Vesala, T.: Testing the applicability of neural networks as a gap-filling method using CH$_4$ flux data from high latitude wetlands, Biogeosciences, 10, 8185–8200, https://doi.org/10.5194/bg-10-8185-2013, 2013.

Dillon, P. J. and Molot, L. A.: Dissolved organic and inorganic carbon mass balances in central Ontario lakes, Biogeochemistry, 36, 29–42, https://doi.org/10.1023/A:1005731828660, 1997.

Duarte, C. M. and Prairie, Y. T.: Prevalence of Heterotrophy and Atmospheric CO$_2$ Emissions from Aquatic Ecosystems, Ecosystems, 8, 862–870, https://doi.org/10.1007/s10021-005-0177-4, 2005.

Eugster, W.: CO$_2$ exchange between air and water in an Arctic Alaskan and midlatitude Swiss lake: Importance of convective mixing, J. Geophys. Res., 108, 4362, https://doi.org/10.1029/2002JD002653, 2003.

Eugster, W., DelSontro, T., and Sobek, S.: Eddy covariance flux measurements confirm extreme CH$_4$ emissions from a Swiss hydropower reservoir and resolve their short-term variability, Biogeosciences, 8, 2815–2831, https://doi.org/10.5194/bg-8-2815-2011, 2011.

Fan, S.-M., Wofsy, S. C., Bakwin, P. S., Jacob, D. J., and Fitzjarrald, D. R.: Atmosphere-biosphere exchange of CO$_2$ and O3 in the central Amazon Forest, J. Geophys. Res.-Atmos., 95, 16851–16864, https://doi.org/10.1029/JD095iD10p16851, 1990.

Finkelstein, P. L. and Sims, P. F.: Sampling error in eddy correlation flux measurements, J. Geophys. Res.-Atmos., 106, 3503–3509, https://doi.org/10.1029/2000JD900731, 2001.

Foken, T. and Wichura, B.: Tools for quality assessment of surface-based flux measurements, Agr. Forest Meteorol., 78, 83–105, 1996.

Forbrich, I., Kutzbach, L., Wille, C., Becker, T., Wu, J., and Wilmking, M.: Cross-evaluation of measurements of peatland methane emissions on microform and ecosystem scales using high-resolution landcover classification and source weight modelling, Agr. Forest Meteorol., 151, 864–874, https://doi.org/10.1016/j.agrformet.2011.02.006, 2011.

Friborg, T., Christensen, T. R., and Søgaard, H.: Rapid response of greenhouse gas emission to early spring thaw in a subarctic mire as shown by micrometeorological techniques, Geophys. Res. Lett., 24, 3061–3064, https://doi.org/10.1029/97GL03024, 1997.

Gažovič, M., Kutzbach, L., Schreiber, P., Wille, C., and Wilmking, M.: Diurnal dynamics of CH$_4$ from a boreal peatland during snowmelt, Tellus B, 62, 133–139, https://doi.org/10.1111/j.1600-0889.2010.00455.x, 2010.

Greenbank, J.: Limnological conditions in ice-covered lakes, especially as related to winter-kill of fish, Ecol. Monogr., 15, 343–392, https://doi.org/10.2307/1948427, 1945.

Greene, S., Walter Anthony, K. M., Archer, D., Sepulveda-Jauregui, A., and Martinez-Cruz, K.: Modeling the impediment of methane ebullition bubbles by seasonal lake ice, Biogeosciences, 11, 6791–6811, https://doi.org/10.5194/bg-11-6791-2014, 2014.

Hargreaves, K. J., Fowler, D., Pitcairn, C. E. R., and Aurela, M.: Annual methane emission from Finnish mires estimated from eddy covariance campaign measurements, Theor. Appl. Climatol., 70, 203–213, 2001.

Horst, T. W.: A simple formula for attenuation of eddy fluxes measured with first-order-response scalar sensors, Bound.-Layer Meteorol., 82, 219–233, https://doi.org/10.1023/A:1000229130034, 1997.

Huotari, J., Ojala, A., Peltomaa, E., Nordbo, A., Launiainen, S., Pumpanen, J., Rasilo, T., Hari, P., and Vesala, T.: Long-term direct CO$_2$ flux measurements over a boreal lake: Five years of eddy covariance data, Geophys. Res. Lett., 38, L18401, https://doi.org/10.1029/2011GL048753, 2011.

Ibrom, A., Dellwik, E., Flyvbjerg, H., Jensen, N. O., and Pilegaard, K.: Strong low-pass filtering effects on water vapour flux measurements with closed-path eddy correlation systems, Agr. Forest Meteorol., 147, 140–156, https://doi.org/10.1016/j.agrformet.2007.07.007, 2007.

Jackowicz-Korczyński, M., Christensen, T. R., Bäckstrand, K., Crill, P., Friborg, T., Mastepanov, M., and Ström, L.: Annual cycle of methane emission from a subarctic peatland, J. Geophys. Res., 115, G02009, https://doi.org/10.1029/2008JG000913, 2010.

Jammet, M., Crill, P., Dengel, S., and Friborg, T.: Large methane emissions from a subarctic lake during spring thaw: Mechanisms and landscape significance, J. Geophys. Res.-Biogeosci., 120, 2015JG003137, https://doi.org/10.1002/2015JG003137, 2015.

Järvi, L., Nordbo, A., Junninen, H., Riikonen, A., Moilanen, J., Nikinmaa, E., and Vesala, T.: Seasonal and annual variation of carbon dioxide surface fluxes in Helsinki, Finland, in 2006–2010, Atmos. Chem. Phys., 12, 8475–8489, https://doi.org/10.5194/acp-12-8475-2012, 2012.

Joabsson, A. and Christensen, T. R.: Methane emissions from wetlands and their relationship with vascular plants: an Arctic example, Glob. Change Biol., 7, 919–932, https://doi.org/10.1046/j.1354-1013.2001.00044.x, 2001.

Johansson, T., Malmer, N., Crill, P. M., Friborg, T., Åkerman, J. H., Mastepanov, M., and Christensen, T. R.: Decadal vegetation changes in a northern peatland, greenhouse gas fluxes and net radiative forcing, Glob. Change Biol., 12, 2352–2369, https://doi.org/10.1111/j.1365-2486.2006.01267.x, 2006.

Jonsson, A., Åberg, J., Lindroth, A., and Jansson, M.: Gas transfer rate and CO$_2$ flux between an unproductive lake and the atmosphere in northern Sweden, J. Geophys. Res.-Biogeosci., 113, G04006, https://doi.org/10.1029/2008JG000688, 2008.

Joyce, J. and Jewell, P. W.: Physical controls on methane ebullition from reservoirs and lakes, Environ. Eng. Geosci., 9, 167–178, https://doi.org/10.2113/9.2.167, 2003.

Kankaala, P., Huotari, J., Peltomaa, E., Saloranta, T., and Ojala, A.: Methanotrophic activity in relation to methane efflux and total heterotrophic bacterial production in a stratified, humic, boreal lake, Limnol. Oceanogr., 51, 1195–1204, https://doi.org/10.4319/lo.2006.51.2.1195, 2006.

Karlsson, J., Ask, J., and Jansson, M.: Winter respiration of allochthonous and autochthonous organic carbon in a subarctic clear-water lake, Limnol. Oceanogr., 53, 948–954, https://doi.org/10.4319/lo.2008.53.3.0948, 2008.

Karlsson, J., Giesler, R., Persson, J., and Lundin, E.: High emission of carbon dioxide and methane during ice thaw in high latitude lakes, Geophys. Res. Lett., 40, 1123–1127, https://doi.org/10.1002/grl.50152, 2013.

Kayranli, B., Scholz, M., Mustafa, A., and Hedmark, Å.: Carbon Storage and Fluxes within Freshwater Wetlands: a Critical Review, Wetlands, 30, 111–124, https://doi.org/10.1007/s13157-009-0003-4, 2009.

Kelly, C. A. and Chynoweth, D. P.: The contributions of temperature and of the input of organic matter in controlling rates of sediment methanogenesis, Limnol. Oceanogr., 26, 891–897, https://doi.org/10.4319/lo.1981.26.5.0891, 1981.

Kirillin, G., Leppäranta, M., Terzhevik, A., Granin, N., Bernhardt, J., Engelhardt, C., Efremova, T., Golosov, S., Palshin, N., Sherstyankin, P., Zdorovennova, G., and Zdorovennov, R.: Physics of seasonally ice-covered lakes: a review, Aquat. Sci., 74, 659–682, https://doi.org/10.1007/s00027-012-0279-y, 2012.

Kirschke, S., Bousquet, P., Ciais, P., Saunois, M., Canadell, J. G., Dlugokencky, E. J., Bergamaschi, P., Bergmann, D., Blake, D. R., Bruhwiler, L., Cameron-Smith, P., Castaldi, S., Chevallier, F., Feng, L., Fraser, A., Heimann, M., Hodson, E. L., Houweling, S., Josse, B., Fraser, P. J., Krummel, P. B., Lamarque, J.-F., Langenfelds, R. L., Le Quéré, C., Naik, V., O'Doherty, S., Palmer, P. I., Pison, I., Plummer, D., Poulter, B., Prinn, R. G., Rigby, M., Ringeval, B., Santini, M., Schmidt, M., Shindell, D. T., Simpson, I. J., Spahni, R., Steele, L. P., Strode, S. A., Sudo, K., Szopa, S., van der Werf, G. R., Voulgarakis, A., van Weele, M., Weiss, R. F., Williams, J. E., and Zeng, G.: Three decades of global methane sources and sinks, Nat. Geosci., 6, 813–823, https://doi.org/10.1038/ngeo1955, 2013.

Kljun, N., Calanca, P., Rotach, M. W., and Schmid, H. P.: A simple two-dimensional parameterisation for Flux Footprint Prediction (FFP), Geosci. Model Dev., 8, 3695–3713, https://doi.org/10.5194/gmd-8-3695-2015, 2015.

Kokfelt, U., Reuss, N., Struyf, E., Sonesson, M., Rundgren, M., Skog, G., Rosén, P., and Hammarlund, D.: Wetland development, permafrost history and nutrient cycling inferred from late Holocene peat and lake sediment records in subarctic Sweden, J. Paleolimnol., 44, 327–342, https://doi.org/10.1007/s10933-010-9406-8, 2010.

Kowalski, C. J.: On the Effects of Non-Normality on the Distribution of the Sample Product-Moment Correlation Coefficient, J. R. Stat. Soc. Ser. C Appl. Stat., 21, 1–12, https://doi.org/10.2307/2346598, 1972.

Lai, D. Y. F.: Methane Dynamics in Northern Peatlands: A Review, Pedosphere, 19, 409–421, https://doi.org/10.1016/S1002-0160(09)00003-4, 2009.

Laurion, I., Vincent, W. F., MacIntyre, S., Retamal, L., Dupont, C., Francus, P., and Pienitz, R.: Variability in greenhouse gas emissions from permafrost thaw ponds, Limnol. Oceanogr., 55, 115–133, https://doi.org/10.4319/lo.2010.55.1.0115, 2010.

Lee, X., Massman, W., and Law, B. (Eds.): Handbook of micrometeorology: A guide for surface flux measurements and analysis, Springer Netherlands., 2005.

Lohila, A., Tuovinen, J.-P., Hatakka, J., Aurela, M., Vuorenmaa, J., Haakana, M., and Laurila, T.: Carbon dioxide and energy fluxes over a northern boreal lake, Boreal Environ. Res., 20, 474–488, 2015.

Lundin, E. J., Giesler, R., Persson, A., Thompson, M. S., and Karlsson, J.: Integrating carbon emissions from lakes and streams in a subarctic catchment, J. Geophys. Res.-Biogeosci., 118, 1200–1207, https://doi.org/10.1002/jgrg.20092, 2013.

Lundin, E. J., Klaminder, J., Bastviken, D., Olid, C., Hansson, S. V., and Karlsson, J.: Large difference in carbon emission – burial balances between boreal and arctic lakes, Sci. Rep., 5, 14248, https://doi.org/10.1038/srep14248, 2015.

Maberly, S. C.: Diel, episodic and seasonal changes in pH and concentrations of inorganic carbon in a productive lake, Freshw. Biol., 35, 579–598, https://doi.org/10.1111/j.1365-2427.1996.tb01770.x, 1996.

Maberly, S. C., Barker, P. A., Stott, A. W., and Ville, M. M. D.: Catchment productivity controls CO$_2$ emissions from lakes, Nat. Clim. Change, 3, 391–394, https://doi.org/10.1038/nclimate1748, 2013.

MacIntyre, S., Jonsson, A., Jansson, M., Aberg, J., Turney, D. E., and Miller, S. D.: Buoyancy flux, turbulence, and the gas transfer coefficient in a stratified lake, Geophys. Res. Lett., 37, L24604, https://doi.org/10.1029/2010GL044164, 2010.

Malmer, N., Johansson, T., Olsrud, M., and Christensen, T. R.: Vegetation, climatic changes and net carbon sequestration in a North-Scandinavian subarctic mire over 30 years, Glob. Change Biol., 11, 1895–1909, https://doi.org/10.1111/j.1365-2486.2005.01042.x, 2005.

Mammarella, I., Nordbo, A., Rannik, Ü., Haapanala, S., Levula, J., Laakso, H., Ojala, A., Peltola, O., Heiskanen, J., Pumpanen, J., and Vesala, T.: Carbon dioxide and energy fluxes over a small boreal lake in Southern Finland, J. Geophys. Res.-Biogeosci., 120, 1296–1314, https://doi.org/10.1002/2014JG002873, 2015.

Mattson, M. D. and Likens, G. E.: Air pressure and methane fluxes, Nature, 347, 718–719, https://doi.org/10.1038/347718b0, 1990.

Mauder, M. and Foken, T.: Impact of post-field data processing on eddy covariance flux estimates and energy balance closure, Meteorol. Z., 15, 597–609, https://doi.org/10.1127/0941-2948/2006/0167, 2006.

Michmerhuizen, C. M., Striegl, R. G., and McDonald, M. E.: Potential methane emission from north-temperate lakes following ice melt, Limnol. Oceanogr., 41, 985–991, https://doi.org/10.4319/lo.1996.41.5.0985, 1996.

Moffat, A. M., Papale, D., Reichstein, M., Hollinger, D. Y., Richardson, A. D., Barr, A. G., Beckstein, C., Braswell, B. H., Churkina, G., Desai, A. R., Falge, E., Gove, J. H., Heimann, M., Hui, D., Jarvis, A. J., Kattge, J., Noormets, A., and Stauch, V. J.: Comprehensive comparison of gap-filling techniques for eddy covariance net carbon fluxes, Agr. Forest Meteorol., 147, 209–232, https://doi.org/10.1016/j.agrformet.2007.08.011, 2007.

Moffat, A. M., Beckstein, C., Churkina, G., Mund, M., and Heimann, M.: Characterization of ecosystem responses to climatic controls using artificial neural networks, Glob. Change Biol., 16, 2737–2749, https://doi.org/10.1111/j.1365-2486.2010.02171.x, 2010.

Moncrieff, J., Clement, R., Finnigan, J., and Meyers, T.: Averaging, detrending, and filtering of eddy covariance time series, in Handbook of Micrometeorology, edited by: Lee, X., Massman, W., and Law, B., 7–31, Kluwer Academic Publishers, The Netherlands, 2004.

Moncrieff, J. B., Malhi, Y., and Leuning, R.: The propagation of errors in long-term measurements of land-atmosphere fluxes of carbon and water, Glob. Change Biol., 2, 231–240, https://doi.org/10.1111/j.1365-2486.1996.tb00075.x, 1996.

Moncrieff, J. B., Massheder, J. M., deBruin, H., Elbers, J., Friborg, T., Heusinkveld, B., Kabat, P., Scott, S., Soegaard, H., Verhoef, A., Moncrieff, J. B., Massheder, J. M., deBruin, H., Elbers, J., Friborg, T., Heusinkveld, B., Kabat, P., Scott, S., Soegaard, H., and Verhoef, A.: A system to measure surface fluxes of momentum, sensible heat, water vapour and carbon dioxide, J. Hydrol., 188–189, 589–611, https://doi.org/10.1016/S0022-1694(96)03194-0, 1997.

Myhre, G., Shindell, D., Bréon, F.-M., Collins, W., Fuglestvedt, J., Huang, J., Koch, D., Lamarque, J.-F., Lee, D., Mendoza, B., Nakajima, T., Robock, A., Stephens, G., Takemura, T., and Zhang, H.: Anthropogenic and Natural Radiative Forcing, in Climate Change 2013: The Physical Science Basis. Contribution of Working Group I to the Fifth Assessment Report of the Inter-

governmental Panel on Climate Change, edited by: Stocker, T. F., Qin, D., Plattner, G.-K., Tignor, M., Allen, S. K., Boschung, J., Nauels, A., Xia, Y., Bex, V., and Midgley, P. M., 659–740, Cambridge University Press, Cambridge, UK and New York, NY, USA, 2013.

Nakai, T., van der Molen, M. K., Gash, J. H. C., and Kodama, Y.: Correction of sonic anemometer angle of attack errors, Agr. Forest Meteorol., 136, 19–30, https://doi.org/10.1016/j.agrformet.2006.01.006, 2006.

Nordbo, A., Launiainen, S., Mammarella, I., Leppäranta, M., Huotari, J., Ojala, A., and Vesala, T.: Long-term energy flux measurements and energy balance over a small boreal lake using eddy covariance technique, J. Geophys. Res., 116, D02119, https://doi.org/10.1029/2010JD014542, 2011.

Olefeldt, D., and Roulet, N. T.: Effects of permafrost and hydrology on the composition and transport of dissolved organic carbon in a subarctic peatland complex, J. Geophys. Res.-Biogeosci., 117, G01005, https://doi.org/10.1029/2011JG001819, 2012.

Olefeldt, D., Turetsky, M. R., Crill, P. M., and McGuire, A. D.: Environmental and physical controls on northern terrestrial methane emissions across permafrost zones, Glob. Change Biol., 19, 589–603, https://doi.org/10.1111/gcb.12071, 2013.

Pacheco, F. S., Roland, F., and Downing, J. A.: Eutrophication reverses whole-lake carbon budgets, Inland Waters, 4, 41–48, https://doi.org/10.5268/IW-4.1.614, 2013.

Papale, D. and Valentini, R.: A new assessment of European forests carbon exchanges by eddy fluxes and artificial neural network spatialization, Glob. Change Biol., 9, 525–535, https://doi.org/10.1046/j.1365-2486.2003.00609.x, 2003.

Papale, D., Reichstein, M., Aubinet, M., Canfora, E., Bernhofer, C., Kutsch, W., Longdoz, B., Rambal, S., Valentini, R., Vesala, T., and Yakir, D.: Towards a standardized processing of Net Ecosystem Exchange measured with eddy covariance technique: algorithms and uncertainty estimation, Biogeosciences, 3, 571–583, https://doi.org/10.5194/bg-3-571-2006, 2006.

Phelps, A. R., Peterson, K. M., and Jeffries, M. O.: Methane efflux from high-latitude lakes during spring ice melt, J. Geophys. Res.-Atmos., 103, 29029–29036, https://doi.org/10.1029/98JD00044, 1998.

Podgrajsek, E., Sahlée, E., and Rutgersson, A.: Diurnal cycle of lake methane flux, J. Geophys. Res.-Biogeosci., 119, 236–248, https://doi.org/10.1002/2013JG002327, 2014.

Podgrajsek, E., Sahlée, E., and Rutgersson, A.: Diel cycle of lake-air CO$_2$ flux from a shallow lake and the impact of waterside convection on the transfer velocity, J. Geophys. Res.-Biogeosci., 120, 2014JG002781, https://doi.org/10.1002/2014JG002781, 2015.

Rannik, Ü., Peltola, O., and Mammarella, I.: Random uncertainties of flux measurements by the eddy covariance technique, Atmos. Meas. Tech., 9, 5163–5181, https://doi.org/10.5194/amt-9-5163-2016, 2016.

Reichstein, M., Falge, E., Baldocchi, D., Papale, D., Aubinet, M., Berbigier, P., Bernhofer, C., Buchmann, N., Gilmanov, T., Granier, A., Grünwald, T., Havránková, K., Ilvesniemi, H., Janous, D., Knohl, A., Laurila, T., Lohila, A., Loustau, D., Matteucci, G., Meyers, T., Miglietta, F., Ourcival, J.-M., Pumpanen, J., Rambal, S., Rotenberg, E., Sanz, M., Tenhunen, J., Seufert, G., Vaccari, F., Vesala, T., Yakir, D., and Valentini, R.: On the separation of net ecosystem exchange into assimilation and

ecosystem respiration: review and improved algorithm, Glob. Change Biol., 11, 1424–1439, https://doi.org/10.1111/j.1365-2486.2005.001002.x, 2005.

Richardson, A. D., Hollinger, D. Y., Burba, G. G., Davis, K. J., Flanagan, L. B., Katul, G. G., William Munger, J., Ricciuto, D. M., Stoy, P. C., Suyker, A. E., Verma, S. B., and Wofsy, S. C.: A multi-site analysis of random error in tower-based measurements of carbon and energy fluxes, Agr. Forest Meteorol., 136, 1–18, https://doi.org/10.1016/j.agrformet.2006.01.007, 2006.

Rinne, J., Riutta, T., Pihlatie, M., Aurela, M., Haapanala, S., Tuovinen, J.-P., Tuittila, E.-S. and Vesala, T.: Annual cycle of methane emission from a boreal fen measured by the eddy covariance technique, Tellus B, 59, 449–457, doi:10.1111/j.1600-0889.2007.00261.x, 2007.

Rudd, J. W. M. and Hamilton, R. D.: Methane cycling in a eutrophic shield lake and its effects on whole lake metabolism, Limnol. Oceanogr., 23, 337–348, https://doi.org/10.4319/lo.1978.23.2.0337, 1978.

Schubert, C. J., Diem, T., and Eugster, W.: Methane emissions from a small wind shielded lake determined by eddy covariance, flux chambers, anchored funnels, and boundary model calculations: A comparison, Environ. Sci. Technol., 46, 4515–4522, https://doi.org/10.1021/es203465x, 2012.

Sebacher, D. I., Harriss, R. C., and Bartlett, K. B.: Methane flux across the air-water interface: air velocity effects, Tellus B, 35B, 103–109, https://doi.org/10.1111/j.1600-0889.1983.tb00014.x, 1983.

Sepulveda-Jauregui, A., Walter Anthony, K. M., Martinez-Cruz, K., Greene, S., and Thalasso, F.: Methane and carbon dioxide emissions from 40 lakes along a north–south latitudinal transect in Alaska, Biogeosciences, 12, 3197–3223, https://doi.org/10.5194/bg-12-3197-2015, 2015.

Serreze, M. C. and Barry, R. G.: Processes and impacts of Arctic amplification: A research synthesis, Glob. Planet. Change, 77, 85–96, https://doi.org/10.1016/j.gloplacha.2011.03.004, 2011.

Shao, C., Chen, J., Stepien, C. A., Chu, H., Ouyang, Z., Bridgeman, T. B., Czajkowski, K. P., Becker, R. H., and John, R.: Diurnal to annual changes in latent, sensible heat and CO$_2$ fluxes over a Laurentian Great Lake: A case study in western Lake Erie, J. Geophys. Res.-Biogeosci., 120, 1587–1604, https://doi.org/10.1002/2015JG003025, 2015.

Sievers, J., Papakyriakou, T., Larsen, S. E., Jammet, M. M., Rysgaard, S., Sejr, M. K., and Sørensen, L. L.: Estimating surface fluxes using eddy covariance and numerical ogive optimization, Atmos. Chem. Phys., 15, 2081–2103, https://doi.org/10.5194/acp-15-2081-2015, 2015.

Smith, L. C., Sheng, Y., and MacDonald, G. M.: A first pan-Arctic assessment of the influence of glaciation, permafrost, topography and peatlands on northern hemisphere lake distribution, Permafrost Periglac., 18, 201–208, https://doi.org/10.1002/ppp.581, 2007.

Sobek, S., Tranvik, L. J., and Cole, J. J.: Temperature independence of carbon dioxide supersaturation in global lakes, Global Biogeochem. Cy., 19, GB2003, https://doi.org/10.1029/2004GB002264, 2005.

Striegl, R. G. and Michmerhuizen, C. M.: Hydrologic influence on methane and carbon dioxide dynamics at two north-central Minnesota lakes, Limnol. Oceanogr., 43, 1519–1529, https://doi.org/10.4319/lo.1998.43.7.1519, 1998.

Tank, S. E., Lesack, L. F. W., and Hesslein, R. H.: Northern delta lakes as summertime CO$_2$ absorbers within the Arctic landscape., Ecosystems, 12, 144–157, https://doi.org/10.1007/s10021-008-9213-5, 2009.

Tranvik, L. J., Downing, J. A., Cotner, J. B., Loiselle, S. A., Striegl, R. G., Ballatore, T. J., Dillon, P., Finlay, K., Fortino, K., Knoll, L. B., Kortelainen, P. L., Kutser, T., Larsen, S., Laurion, I., Leech, D. M., McCallister, S. L., McKnight, D. M., Melack, J. M., Overholt, E., Porter, J. A., Prairie, Y., Renwick, W. H., Roland, F., Sherman, B. S., Schindler, D. W., Sobek, S., Tremblay, A., Vanni, M. J., Verschoor, A. M., von Wachenfeldt, E., and Weyhenmeyer, G. A.: Lakes and reservoirs as regulators of carbon cycling and climate, Limnol. Oceanogr., 54, 2298–2314, https://doi.org/10.4319/lo.2009.54.6_part_2.2298, 2009.

Varadharajan, C. and Hemond, H. F.: Time-series analysis of high-resolution ebullition fluxes from a stratified, freshwater lake, J. Geophys. Res.-Biogeosci., 117, https://doi.org/10.1029/2011JG001866, 2012.

Verpoorter, C., Kutser, T., Seekell, D. A., and Tranvik, L. J.: A global inventory of lakes based on high-resolution satellite imagery, Geophys. Res. Lett., 41, 6396–6402, https://doi.org/10.1002/2014GL060641, 2014.

Vesala, T., Huotari, J., Rannik, Ü., Suni, T., Smolander, S., Sogachev, A., Launiainen, S., and Ojala, A.: Eddy covariance measurements of carbon exchange and latent and sensible heat fluxes over a boreal lake for a full open-water period, J. Geophys. Res., 111, D11101, https://doi.org/10.1029/2005JD006365, 2006.

Vickers, D. and Mahrt, L.: Quality control and flux sampling problems for tower and aircraft data, J. Atmos. Ocean. Tech., 14, 512–526, 1997.

Vonk, J. E., Tank, S. E., Bowden, W. B., Laurion, I., Vincent, W. F., Alekseychik, P., Amyot, M., Billet, M. F., Canário, J., Cory, R. M., Deshpande, B. N., Helbig, M., Jammet, M., Karlsson, J., Larouche, J., MacMillan, G., Rautio, M., Walter Anthony, K. M., and Wickland, K. P.: Reviews and syntheses: Effects of permafrost thaw on Arctic aquatic ecosystems, Biogeosciences, 12, 7129–7167, https://doi.org/10.5194/bg-12-7129-2015, 2015.

Walter, K. M., Zimov, S. A., Chanton, J. P., Verbyla, D., and Chapin, F. S.: Methane bubbling from Siberian thaw lakes as a positive feedback to climate warming, Nature, 443, 71–75, https://doi.org/10.1038/nature05040, 2006.

Walter, K. M., Chanton, J. P., Chapin, F. S., Schuur, E. A. G., and Zimov, S. A.: Methane production and bubble emissions from arctic lakes: Isotopic implications for source pathways and ages, J. Geophys. Res.-Biogeosci., 113, G00A08, https://doi.org/10.1029/2007JG000569, 2008.

Walter Anthony, K., Daanen, R., Anthony, P., Schneider von Deimling, T., Ping, C.-L., Chanton, J. P., and Grosse, G.: Methane emissions proportional to permafrost carbon thawed in Arctic lakes since the 1950s, Nat. Geosci., 9, 679–682, https://doi.org/10.1038/ngeo2795, 2016.

Wanninkhof, R., Ledwell, J. R., and Broecker, W. S.: Gas exchange-wind speed relation measured with sulfur hexafluoride on a lake, Science, 227, 1224–1226, https://doi.org/10.1126/science.227.4691.1224, 1985.

Webb, E. K., Pearman, G. I., and Leuning, R.: Correction of flux measurements for density effects due to heat and water vapour transfer, Q. J. Roy. Meteor. Soc., 106, 85–100, https://doi.org/10.1002/qj.49710644707, 1980.

Wetzel, R. G.: Limnology?: lake and river ecosystems, 3rd ed., Academic Press, San Diego, CA, 1006 pp., 2001.

Weyhenmeyer, G. A., Kosten, S., Wallin, M. B., Tranvik, L. J., Jeppesen, E., and Roland, F.: Significant fraction of CO$_2$ emissions from boreal lakes derived from hydrologic inorganic carbon inputs, Nat. Geosci., 8, 933–936, https://doi.org/10.1038/ngeo2582, 2015.

Whiting, G. J. and Chanton, J. P.: Greenhouse carbon balance of wetlands: methane emission versus carbon sequestration, Tellus B, 53, 521–528, https://doi.org/10.1034/j.1600-0889.2001.530501.x, 2001.

Wik, M., Crill, P. M., Bastviken, D., Danielsson, Å., and Norbäck, E.: Bubbles trapped in arctic lake ice: Potential implications for methane emissions, J. Geophys. Res., 116, G03044, https://doi.org/10.1029/2011JG001761, 2011.

Wik, M., Crill, P. M., Varner, R. K., and Bastviken, D.: Multiyear measurements of ebullitive methane flux from three subarctic lakes, J. Geophys. Res.-Biogeosci., 118, 1307–1321, https://doi.org/10.1002/jgrg.20103, 2013.

Wik, M., Thornton, B. F., Bastviken, D., MacIntyre, S., Varner, R. K., and Crill, P. M.: Energy input is primary controller of methane bubbling in subarctic lakes, Geophys. Res. Lett., 41, 555–560, https://doi.org/10.1002/2013GL058510, 2014.

Wik, M., Varner, R. K., Anthony, K. W., MacIntyre, S., and Bastviken, D.: Climate-sensitive northern lakes and ponds are critical components of methane release, Nat. Geosci., 9, 99–105, https://doi.org/10.1038/ngeo2578, 2016.

Wilczak, J. M., Oncley, S. P., and Stage, S. A.: Sonic anemometer tilt correction algorithms, Bound.-Layer Meteorol., 99, 127–150, https://doi.org/10.1023/A:1018966204465, 2001.

Wille, C., Kutzbach, L., Sachs, T., Wagner, D., and Pfeiffer, E.-M.: Methane emission from Siberian arctic polygonal tundra: eddy covariance measurements and modeling, Glob. Change Biol., 14, 1395–1408, https://doi.org/10.1111/j.1365-2486.2008.01586.x, 2008.

Yvon-Durocher, G., Allen, A. P., Bastviken, D., Conrad, R., Gudasz, C., St-Pierre, A., Thanh-Duc, N., and del Giorgio, P. A.: Methane fluxes show consistent temperature dependence across microbial to ecosystem scales, Nature, 507, 488–491, https://doi.org/10.1038/nature13164, 2014.

Zeikus, J. G. and Winfrey, M. R.: Temperature limitation of methanogenesis in aquatic sediments., Appl. Environ. Microbiol., 31, 99–107, 1976.